www.elsevier.com/locate/dsr2

An introduction to the physical oceanography of six seamounts in the southwest Indian ocean

Jane Read, Raymond Pollard

PII: S0967-0645(15)00224-6
DOI: http://dx.doi.org/10.1016/j.dsr2.2015.06.022
Reference: DSRII3918

To appear in: *Deep-Sea Research II*

Cite this article as: Jane Read, Raymond Pollard, An introduction to the physical oceanography of six seamounts in the southwest Indian ocean, *Deep-Sea Research II,* http://dx.doi.org/10.1016/j.dsr2.2015.06.022

An introduction to the physical oceanography of six seamounts in the Southwest Indian Ocean

Jane Read[1]*, Raymond Pollard[1]

[1]National Oceanography Centre, University of Southampton Waterfront Campus, European Way, Southampton, SO14 3ZH, UK

*Corresponding author, email address: janefread@gmail.com

telephone: +44 1590682118

Abstract

Exploratory surveys of six seamounts in the Southwest Indian Ocean provide a description of physical processes induced by seamounts along the Southwest Indian Ridge. Mean currents (15-25 cm s^{-1}) in the vicinity of each seamount were dominated by mesoscale eddies. The dominant seamount-driven process was the generation of internal tides by the barotropic tide interacting with the seamount crests. This led to enhanced shear in the vicinity of the crests resulting in mixing where stratification was weak, for example in the core of an anticyclonic mesoscale eddy or where there had been a winter mixed layer. Tidally driven up- and downwelling was observed at the seabed with associated variability in bottom temperature of up to 3°C over a tidal cycle. Vertical displacement of isopycnals by internal tidal waves reached 200 m peak to trough. Fluorescence in the surface (eutrophic) layer could thus extend down to the seamount crest on each tidal cycle. Apparently spatial variations in short conductivity/temperature/depth sections across each seamount were probably aliased temporal variations from the strong tidal signal. Evidence for Taylor caps or other potential trapped circulations at the seamount crest was weak, most likely because currents associated with mesoscale eddies were too strong to allow their formation.

Keywords: Southwest Indian Ridge, seamounts, ocean circulation, internal tides

1. Introduction

Seamounts are isolated topographic features, rising relatively steeply from the deep-sea floor. Such features impact ocean circulation, interacting with large-scale flows, converting ocean tidal energy to smaller scales, and creating turbulence that affects local and global circulation as well as impacting on biological response. Seamounts have been hypothesised to be hotspots of biological biodiversity and productivity (Clark et al., 2010; Rogers, 1994; Rowden et al., 2010) and the physical processes associated with seamounts are thought to impact the local fauna and flora in several different ways. Many of the paradigms have been questioned (Genin and Dower, 2007; Rowden et al., 2010) and the evidence is mixed (White et al., 2007), but there is little doubt that physical oceanography can play an important role in the distribution of fauna and flora (Genin, 2004; Shank, 2010). Therefore, when a first investigation took place into the deep-sea biology of selected seamounts of the Southwest Indian Ocean, physical observations were made as well. Acoustic studies of fish and zooplankton distribution and bathymetric swath mapping were made alongside measurements of upper ocean currents and full depth profiling of physical parameters. Because of the constraints imposed by multi-disciplinary collaborative work, the physical oceanography measurements were sufficient to provide a description of some of the likely processes operating but were inadequate to fully quantify them.

Physical processes induced by seamounts and their biological consequences have been recently reviewed (Lavelle and Mohn, 2010; White et al., 2007), so need be only briefly introduced here. The passage of a steady current over a seamount can induce a Taylor column or cap, an isolated region of water trapped above the topography (Hogg, 1973) which has been hypothesised to influence the distribution of biota by retention of plankton over the summit (White et al., 2007). If currents are too large, a Taylor cap will not form. Seamounts are also impacted by periodic flows, with semi-diurnal tidal oscillations dominating the Nansen observations. Because these tides have a shorter period than the local inertial period (18 - 23 hours at the seamounts observed during Nansen, Table 1), they can exist as free internal waves. Thus the barotropic (depth independent) semidiurnal tidal flow, impinging on the seamount topography, generates internal tides, leading to vertical motions and possibly mixing in the vicinity of the seamount.

Substantial internal tides can be generated over rough topography such as ridges and seamounts. These internal tides play an important role in deep ocean mixing. The global thermohaline circulation results from the balance between sinking cold water in polar regions and the mixing upwards of cold water at lower latitudes. The global energy requirement for this mixing is about 2 terawatts (1 terawatt = 10^{12}W) (Garrett, 2003). Analysis of altimetric sea surface height shows the western Indian Ocean to be a region of enhanced dissipation, in particular the Mascerene and Southwest Indian Ridges and the Madagascar Plateau are major source regions (Egbert and Ray, 2001). Therefore it is important to understand the role seamounts play in interacting with tides and the generation of internal waves that dissipate tidal energy through the mixing and vertical redistribution of heat in the water column.

In this paper, we overview the circulation of the Southwest Indian Ocean then examine the physical behaviour at each seamount. Finally, we summarise the evidence for several processes: Taylor columns; rectified flow; generation of internal tides and mixing. We begin by introducing the data collected.

2. Data

The data described here were collected during the RV *Dr Fridtjof Nansen* cruise 2009 410, between 12 November – 19 December 2009 (Rogers et al., 2009). The objectives of the cruise were to understand the pelagic biology and physical oceanographic setting of seamounts on the Southwest Indian Ocean Ridge as part of a larger project to investigate seamount benthic communities, coral diversity and the impact of deep-sea fishing activities (Rogers et al., 2014). Six seamounts were investigated (Fig. 1). Five were along the Southwest Indian Ridge, from north to south these were Atlantis Bank, Sapmer Seamount, Middle of What Seamount, Melville Bank and Coral Seamount. The final seamount was an unnamed feature on the Madagascar Ridge, north west of a large submarine plateau, Walter's Shoals. In this paper we refer to the seamount as Walter Seamount for convenience, but it should be noted that the feature is separate from the plateau and is not officially named.

Physical processes at seamounts are driven by both steady state and periodic flows. To investigate these different flows requires different approaches. In the limited time available, conductivity, temperature and pressure (CTD) sampling consisted of (i) a 24-h CTD yoyo at or close to the seamount summit (with the ship held stationary relative to the seamount) to quantify the periodic flows resulting primarily from tides and (ii) a short, closely spaced, CTD transect across each seamount. Station spacing varied from <1km to ~4km and was designed around the topography, but transect orientation followed the alignment of acoustic mapping of currents using an acoustic Doppler current profiler (ADCP), zooplankton (with a Simrad EK60 multiple transducer array) and bathymetry (using a Simrad EM710 multibeam echosounder) at the same time (Rogers et al., 2014). Survey alignment was designed to optimise acoustic performance allowing for the prevailing weather conditions at the time of each survey. With the multitude of acoustic instruments, data from the ADCP were occasionally compromised. The CTD transects provided information about water masses, cross seamount gradients and steady or slowly varying flows. Two longer CTD transects, across the major current systems south of Melville and Middle of What Seamounts (Fig. 1) were also undertaken. When combined with satellite altimetry, these provided information about the larger scale circulation (Pollard and Read, 2015).

The CTD data were collected with a SeaBird Electronics SBE 9/11+ CTD and deck unit. All profiles were worked to within a few metres of the seabed. Conductivity was calibrated using samples drawn from twelve 5-litre Niskin bottles and analysed on a Guildline Portasal model 8410 using standard seawater batch number P144. Problems were encountered with the calibration (Rogers et al., 2009), but following post cruise re-processing and calibration, salinity is believed to be good to 0.0003 ± 0.005 . A total of 423 stations were worked, the majority during CTD yoyos.

Upper ocean currents were measured throughout the cruise using an RDI Ocean Surveyor 150 kHz ADCP mounted in the ship's hull. The instrument was configured with 100 8-metre bins, of which the top 50 were meaningful. Individual pings were corrected internally for ship's heading using the 1-second NMEA input from the Seatex Seapath 200. Data were averaged internally over 3 minutes and 20 minutes. No calibration for misalignment angle was attempted during the cruise. However, the first acoustic survey provided coherent data (with neither convergence or divergence of a steady, unidirectional, flow) over a grid indicating that any misalignment angle must be small. Current data gathered during the 24-h CTD

yoyo period were decomposed into barotropic and baroclinic components. The depth-averaged current formed the barotropic component and the baroclinic component consisted of the deviation from this (Park et al., 2008).

Maps of sea surface height (mean absolute dynamic topography, MADT) were obtained from the Segment Sol multimissions d'ALTimétrie, d'Orbitographie et de localisation precise/Developing Use of Altimetry for Climate Studies (SSALTO/DUACS) multimission altimeter data processing system of Collecte Localis Satellites/Archivage, Validation, Interprétation des données des Satellite Océanographiques) (CLS/AVISO).

The mapped product was created from 7 days of data merged from all available satellites (Envisat, Jason-1 and Jason-2) gridded at 1/3rd degree resolution on a Mercator grid.

Maps of chlorophyll a were obtained from the NASA Ocean Colour distribution website. Data presented here are Level 3 binned 8-day composites from the Aqua MODIS satellite sensor at 4.6 km resolution.

Predicted tides were obtained from the Egbert tidal model (Egbert and Erofeeva, 2002) using Oregon State University tidal prediction software (OTIS). Elevation and velocity were extracted at the location of the CTD yoyo for each seamount. Mixed tides, with the diurnal tide greater than the semidiurnal component, were found at all sites. This was more pronounced at some seamounts than others and at different times in the lunar month.

3. Situation of seamounts in the large-scale circulation

Satellite altimetry of the Southwest Indian Ocean (overlaid on chlorophyll data in Fig. 2) provided a synoptic overview of the circulation via sea surface height (SSH). The dominant flow in the region is the combined eastward flow of the Subtropical Front (STF) and Agulhas Return Current (ARC), as indicated by the closely spaced, generally west to east SSH contours between 37°S and 42°S (Pollard and Read, 2015). Five of the seamounts were in the subtropical gyre north of this boundary (Table 1, Fig. 1), where the long-term mean return flow is predominantly westwards. One seamount, Coral, was located south of the STF and ARC in the Subantarctic zone and in a region of relatively weak SSH gradient and eastwards flow.

The seamounts spanned over 10 degrees of latitude with surface temperatures ranging from 27°C in the north to 8°C in the south, with the greater part of the difference occurring across the STF and ARC. Upper ocean warm water masses (Fig. 3) included fresh Tropical Surface Water (TSW, >23°C) north of Atlantis Bank, saline Subtropical Surface Water (STSW, 15°C, 35.50 – 24°C, 35.60) and South Indian Central Water (SICW, 8°C, 34.60 – 15°C, 35.50) or Subantarctic Mode Water (SAMW) throughout the subtropical gyre (Read and Pollard, 1993). Colder Subantarctic Surface Water (SASW, 6°C, 34.10 – 8°C, 34.20) was found at Coral Seamount. At intermediate to deep depths, the salinity minimum of Antarctic Intermediate Water (AAIW, 4.5°C, 34.40) was found throughout the survey. At Coral, the salinity minimum occurred between 600-700m, while at all seamounts north of the STF/ARC the salinity minimum of AAIW was found between 1200-1400m. All casts that were deep enough extended into the

deep-water complex (North Atlantic, Indian or Circumpolar Deep Water). Generally the water depth around the seamounts was too shallow to observe deep or bottom water.

In addition to the major fronts (STF and ARC), a north subtropical front at the southern boundary of the upper ocean pool of warm, salty subtropical water of the central South Indian Ocean has been identified (Belkin and Gordon, 1996). They suggest that this front is connected with the Agulhas Front, diverging from it east of 45°E. The feature was also observed in the Fine Resolution Antarctic Model (Sparrow et al., 1996). Throughout the cruise, temperature, salinity and fluorescence were measured nearly continuously. The northern boundary of saline subtropical water was observed at about 22°S. At 40°S a 4°C and 1.0 drop in temperature and salinity marked the presence of the Subtropical Front in close proximity to the Agulhas Return Current. A further decrease of about 3°C and 0.5 between 40° - 41.5°S marked the influence of the Subantarctic Front. There was no evidence of a separate north subtropical front.

Cyclonic and anticyclonic eddies are superimposed on the mean circulation (Pollard and Read, 2015). Both Sapmer and Middle of What were strongly influenced by a large anticyclonic eddy immediately north of the STF and ARC and northwest of Sapmer (centred at 36.5°S, 52°E). South of Madagascar, Walter Seamount was located between a pair of dipole eddies north and south of the seamount, centred at about 31°S, 42°E and 32.5°S, 42.5°E (Fig. 2).

Fig. 2 does not reveal a chlorophyll a signature at any seamount, though it is possible that any such signature is on too small a scale to be resolved by satellite. It is clear, however, that primary productivity is enhanced between the Agulhas Return Current and the Subtropical Front in a band that may be several hundred km wide. Streaks of enhanced chlorophyll a can be seen drawn around the cyclonic eddies that break off the Agulhas Return Current to the north. While Melville, Coral and Middle of What Seamounts all lie close to the fronts, none of them lies in the band of strongest chlorophyll a.

4. Physical oceanography at each seamount

In this section we investigate significant features of the circulation near each seamount.

4.1 Atlantis Bank

Atlantis Bank, located at 32° 42'S, 57° 16'E (Fig. 1), was the only seamount of the six under study to have been previously surveyed (Dick, 1998). However no biological or physical observations were made during the 1988 geological survey. Elongated north to south on a transform ridge along the eastern side of the Atlantis II Fracture Zone, the bank had a wave cut platform at a depth of about 700 m with pinnacles rising to 70 m below the sea surface (Fig. 1c).

Atlantis Bank was situated within the southwest Indian subtropical gyre and altimeter-derived sea surface height showed the region to be an area of weak circulation (Fig. 2). Currents were less than 20 cm s^{-1} in a west to southwest direction. Shipboard ADCP showed similar strength currents, but during the first acoustic survey the pattern of flow was anticyclonic above the seamount. Analysis of the stream function showed this to be confined to the upper 100 m, below which there was a steady southwestward flow of 20 cm s^{-1}.

Mean temperature and salinity of the upper 200 m were 16.56°C, 35.505 and horizontal gradients were weak, except across the seamount below 750 m where isopycnals sloped down from northeast to southwest implying a northwestward baroclinic flow (Fig. 4a). Slight doming of temperature, salinity and density at 700 m over the seamount gave rise to <1°C and <0.10 difference between on and off seamount temperature and salinity respectively. The doming penetrated upwards with diminishing effect (Fig. 4a). The doming may well be a spatial (rather than a temporal) feature because the CTD yoyo (Fig. 4b) showed vertical excursions of isopycnals of similar amplitude. This is discussed further for Melville Bank (section 4.4).

The 24-h CTD yoyo showed more structure with a sequence of three or four pycnoclines in the vertical, each of about 0.1 kg m^{-3} (Fig. 4b). Strength and depth varied due to the passage of internal waves and tides but the pycnoclines were generally at depths of about 30-40 m, 50-60 m, 90-110 m and sometimes 120-150 m . These likely resulted from the development of the mixed layer over a period of time, however they had close correspondence to the current structure. ADCP currents showed layering with stronger currents in regions of greater vertical density gradients and weaker currents where the vertical density gradients were weaker. For example, in Fig. 4c, between 0 - 6 hours at roughly 80 m depth, weak currents were associated with a pycnostad 26.1 - 25.9 kg m^{-3}), similarly between 12 - 18 hours at about 120 m depth, the pycnostad between 26.2 - 26.1 kg m^{-3}) is associated with weak currents.

At the seabed, the depth of the 26.8 kg m^{-3} isopycnal shows a semidiurnal signal of upwelling and downwelling (Fig. 4b). Temperature varied by up to 1°C and salinity by up to 0.1 over a 12 hour period. The effect of upwelling extended up to 100 m above the seabed and during the first 15 hours of the record, was overlain by a region of weak vertical gradients. Density gradients increased with decreasing depth to about 250m depth.

In summary, Atlantis Bank was situated in the subtropical gyre, where the general circulation was weak and currents impinging upon the seamount were similarly weak. The water column was well stratified. There was evidence of tidally driven up- and down-welling, with cooling and freshening then warming and increased salinity in the bottom 200 m over the period of the tidal cycle.

4.2 Sapmer Seamount

Sapmer Seamount was located above the Gallieni Fracture Zone at 36° 51'S, 52° 9'E (Fig. 1). Three buttresses extended southeastwards from the roughly triangular shaped seamount towards the steep slope into the Fracture Zone (Fig. 1e). Altimeter-derived velocities were about 20 cm s^{-1} and sea surface height showed an anticyclonic eddy situated over the seamount and elongated in the northeast-southwest direction parallel to the Agulhas Return Front and STF (Fig. 2). Currents measured by the ADCP were 30-60 cm s^{-1} to the east. The most likely explanation for the discrepancy between altimeter-derived currents and in situ measurements was movement of the eddy, which has been blurred by the merging of 8 days of satellite data.

The most striking feature of Sapmer Seamount was the weak stratification across the top 400 m (Fig. 5). The 50 - 350 m change in salinity was less than 0.02 and potential temperature varied by only 0.3°C. Mean temperature and salinity of the top 200 m across the seamount were 15.82°C, 35.452. This was

cooler and fresher than seamounts to north and south (Atlantis Bank 16.56°C, 35.505 and Middle of What Seamount 16.60°C, 35.548). Prior to arrival at the seamount, the vessel experienced two days of gale force winds (up to 25 m s^{-1}). Despite this, the yoyo does not show a particularly deep well-mixed layer (less than 50 m). So the primary reason for the weak stratification down to 400 m was the presence of the well-developed anticyclonic eddy centred on Sapmer (Pollard and Read, 2015).

Sapmer was subject to a mixed tide, i.e., the semidiurnal component was weaker (8 cm range) than the diurnal signal (24 cm range in tidal height) (Egbert & Erofeeva, 2002). The CTD yoyo (Fig. 5), worked on the southeastern tip of the central buttress, showed internal tides, with elevation of isopycnals occurring twice during the 24-h period. For example, the 26.23 kg m^{-3} isopycnal (Fig. 5c) peaks at 7 and 20 hours into the record and the peak to trough change in height is over 100 m. Associated with this is the appearance of cold water in the bottom 100 m at about the same time as the shallower contours peak and disappears when they slump downwards, e.g. at 15 hours.

It is relevant to note that the peaks in tidal elevation tend to occur later as depth increases. For example, the isopycnal 26.30 kg m^{-3} is shallowest at 10 and 22 hours into the record, 2-3 hours later than the peaks in isopycnal 26.23 kg m^{-3}. Thus the phase of the semidiurnal tide has a downward propagating component. Internal wave energy, which propagates at right angles to the phase (Gill, 1982) must therefore have an upwards vertical component. This indicates that internal tides are forced by the interaction of the barotropic tide and the seamount, so that tidal energy propagates upwards from the seabed. Potential for tidal mixing will thus be greatest near the bottom.

The CTD section across the seamount (not shown) showed no horizontal gradient in isopycnals above 400 m or below 1000 m. Between these two depths there was a horizontal gradient of increasing density from northwest to southeast. Superimposed on this, the isopycnals close to the seamount showed compression and separation in the vertical indicating the possible existence of localised flow around the topography. Compression and separation may also indicate enhanced mixing, which is likely given the very weak stratification. Doming of isotherms and isopycnals over the crest of the seamount show upwelling of water from 50-100 m deeper in the water column. However, given the tidal, vertical excursions seen in the yoyo (Fig. 5), these effects could all be tidal.

The tidal pulse of dense water that appeared about 10 hours into the yoyo (isopycnal 26.30 kg m^{-3}) extended 150-200 m above the seabed (512 m) and resembles the passage of a solitary wave of elevation. These internal waves occur at the interface of a two layer system, where a weakly stratified layer overlies a thin, stratified layer above the seabed (Klymak and Moum, 2003). Such waves can be highly turbulent, leading to increased suspension of benthic material, transport of properties and material and mixing. Unfortunately good ADCP data were limited to 350 m or less, so there is no information about the currents at the seabed at Sapmer and through this feature.

The subtleties of stratification are emphasised by the Brünt-Väisäla frequency which reveals the presence of a weak seasonal pycnocline at 20 - 50 m with depth-varying pycnoclines beneath that correspond to changes in the current field. In the top 350 m, the Brünt-Väisäla frequency is less than 1 cycle per hour (cph) except in the pycnoclines where it increases to 2-3 cph.

Where stratification is weak enough to be broken down by vertical shear, the tendency of a fluid to remain stratified will be overcome leading to the development of small scale vertical turbulent mixing. The tendency is quantified by the Richardson number (Ri, the ratio of the stratification divided by the shear squared). Ri < 0.25 indicates a strong likelihood of mixing, with values < 1 indicating the potential for mixing. Ri is contoured down to 300 m in Fig. 5e, limited to this depth by unreliable ADCP velocities at greater depths.

Vertical shears combined with unusually weak stratification gave rise to significantly low Richardson numbers. Over most of the top 300 m, Ri is < 1.0 and there are a significant number of patches > 50 m in vertical extent where Ri < 0.25. Most of these are either above 150 m or below 200 m, separated by the weak pycnocline around σ_0 = 26.23. Overall, below 100m, Ri < 1.0 more than 70% of the time. Hence it is likely that there was turbulent mixing over the crest of Sapmer Seamount.

We conclude that Sapmer Seamount was (at the time of the survey) dominated by the presence of a large anticyclonic eddy. Upward propagation of tidal energy from the bottom is evidence that internal tides are initiated by the interaction of the barotropic tide and the seamount crest. Tidally driven shear combined with unusually weak stratification gave rise to low Richardson numbers indicating strong potential for turbulent mixing. Upwelling near the seabed was evident from the occurrence of fresher, colder water during the tidal cycle. A pulse of dense water may indicate the passage of a solitary wave of elevation.

4.3 Middle of What Seamount

Middle of What Seamount appeared to have only weak influence on the circulation of the water column. However, it was one of only two seamounts at which full depth lowered ADCP data were collected and the current data showed reversals in flow close to the seabed that appeared to be related to the topography.

Middle of What Seamount was situated on the south side of the mid-axial rift valley of the Southwest Indian Ridge (Fig.1). Unlike the other seamounts on this ridge, it was not associated with a deep fracture zone. The seamount was bisected by a fault running west to east, with a steep scar face caused by the elevation of the south side of the fault (Fig. 1d) (see also bathymetry in Fig. 6 near 50.40°E and 50.43°E). The seamount shallowed to its highest point, 1000 m, immediately above the fault (note that the CTD section did not cross this point therefore the shallowest point does not show in the bathymetry of Fig. 6). Features best described as hills and hummocks, with elevations of up to two hundred metres, were superimposed on the seamount and the surrounding area (Fig. 1d).

Sea surface height (Fig. 2) showed the seamount to be on the northern edge of the Agulhas Return Current and the southern edge of an extensive warm core ring. Sapmer Seamount was in the centre of the same eddy. Altimeter-derived currents were about 25 cm s^{-1} eastwards. The first ADCP grid showed weaker currents of about 20 cm s^{-1} but there was a change during the CTD yoyo and by the time of the second grid survey the currents had increased up to 50 cm s^{-1}.

Watermass properties and distribution were typically subtropical (Fig. 3). During the CTD yoyo (not shown) the upper ocean properties were almost the same as those at Sapmer Seamount, i.e. weakly stratified in the upper 250 m with almost no vertical gradient in salinity and a very weak gradient in temperature. Mean temperature and salinity of the top 200 m were 16.60°C and 35.548 respectively.

Lowered ADCP velocities collected during the CTD section (Fig. 6) show similar vertical structure for each CTD, indicating that tidal currents over the 7 hours taken to complete the section do not swamp spatial changes. The currents appear to be layered in the vertical. In the surface layer down to a pycnocline at 150-180 m, currents were predominantly eastward at about 25 cm s^{-1}. Below that depth the currents rotated to a more southeasterly flow of about 33 cm s^{-1}. Deeper in the water column, between 400 - 600 m depth, flow northwest of the seamount tended to eastwards while that southeast of the seamount continued in a southeasterly direction. There was a further change at about 900m depth below which the currents began to rotate in a clockwise (cyclonic) direction with depth. Below the crest of the seamount, profiles closest to the steep scarps completely reverse in direction, as the currents are constrained to flow parallel to the bottom contours (Fig. 1d).

In addition to the weak stratification in the top 150 m, there is further weak stratification between about 400 - 800 m, with hints of weaker stratification on the flanks of the seamount. Ri was calculated over 10 m intervals to investigate the likelihood of mixing. The results were too patchy to contour but statistically Ri < 1 for about 25% of the estimates (.i.e. 5 values in every 200 m depth interval). In a few areas the percentage Ri < 1 rose to about 50%, and grey bars mark those areas on Fig. 6. In the main, the areas with higher probability of low Ri lie in two bands: across the thermocline below the base of the mixed layer centred on 200 m; and deeper in the water column a few hundred metres above and below the peak of Middle of What Seamount. These areas are not where the stratification is weakest, but more where shear is enhanced. Our conclusion is that, given the relatively weak stratification in the anticyclonic eddy (cf Sapmer), enhanced shear can lead to internal mixing in a significant fraction of the water column. The enhanced shear itself results primarily from internal tides generated by the interaction of the barotropic tide with the seamount. Thus, while the deep seamount may only weakly influence the stratification, it has a significant influence on mixing through the water column.

4.4 Melville Bank

Melville Bank was located at 38° 28'S, 42° 49'E on the eastern side of the Indomed Fracture Zone (Fig. 1). Altimeter-derived velocities were approximately 20 cm s^{-1} to the southwest, while shipboard currents during the survey showed speeds from 40 - 70 cm s^{-1} to the west and southwest. The southwestward flow resulted from the proximity of an eddy breaking off in a meander of the Agulhas Return Current (Fig. 2). The upper ocean was subtropical in character (Fig. 3) with mean temperature and salinity of the top 200 m of 16.28°C and 35.54 respectively. Water mass properties were typical of Subtropical Surface Water overlying South Indian Central Water but with interleaving between 15-16°C at approximately 35.30.

Melville Bank was elongated west to east with a shallowest elevation of about 100 m in the east and a slightly deeper elevation of about 400 m to the west (Fig. 1g). The CTD yoyo was worked between these two, just above a col about 600 m deep on the western shoulder of the shallowest part of the seamount.

Two CTD transects were worked: the first was made from south to north; the second was worked from east to west along the crest of the seamount about 2 days after the first.

On the first section (Fig. 7a) isopycnals were nearly flat between 600 - 800 m depth and sloped up to the north above this, consistent with westward baroclinic flow through the section and agreeing with the velocity data. Above the pycnocline, isopycnals were bowl-shaped, deepest over and south of the seamount, shallowest to the north and south of the section. At the crest of the seamount, isopleths dipped down sharply, with upper ocean water drawn downwards. Thus at 100 m, just above the shallowest point of the seamount (103 m), the water was warmer than that to north or south, by up to 0.8°C. The horizontal gradient was more pronounced to the north than the south, with temperatures at 100m of 16.56°C vs 15.72°C (north) and 16.35°C (south).

Conversely during the second west to east CTD section (Fig. 7b) the isopleths were domed over the crest of the seamount with water at 100 m (15.95°C) up to 0.8°C colder than that to east (16.75°C) or west (16.24°C). A similar, but less extreme feature appeared over the western crest, at 423 m, where the water on the crest of the ridge (13.58°C) was colder by up to 0.4°C than that to east (14.03°C) or west (13.90°C). At the western crest the effect did not reach the surface but displacement of the isopycnals extended upwards for over 100 m.

The change in isopycnal slopes between the two CTD transects leads us to ask whether the changes are temporal rather than spatial. The CTD yoyo showed a semidiurnal signal with the passage of two internal wave crests at about 5 and 17 hours during a 24 hour period, e.g. the 16°C isotherm (Fig. 8), but the first peak was steeper and more pronounced than the second. The Egbert tidal model predicts a mixed dominant semidiurnal tide at Melville Bank (Fig. 9a). The survey took place close to neap tides when the first tide was approximately twice the height of the second (33-37 cm vs 17-19 cm), which might explain the difference in the two internal waves observed. Note that deeper peaks lag the shallower ones, e.g., the 13°C isotherm peaks at 9 and 22 hours. As for Sapmer, upward tidal energy propagation is inferred.

The barotropic tide predicted by the Egbert model is the forcing function for local internal tides. As the barotropic tide interacts with Melville Bank, it generates internal tides that are likely to be proportional in amplitude (close to the Bank) to the barotropic tide but different in phase. Quantifying the internal tide by the pressure (depth) of the density surface σ_0 = 26.2 kg m^{-3} (Fig. 9a), the stronger then weaker internal wave crests during the CTD yoyo reasonably match the phase and differing amplitudes of the v component of the barotropic tide (north velocity, dashed line). The depth of σ_0 = 26.2 kg m^{-3} for all the CTDs in the two sections is also shown on Fig. 9a, plotted at the time of each station. All the CTD section stations lie in close proximity, within a circle of 6 km radius. Despite the sections having been occupied more than five tidal cycles earlier that the start of the yoyo, there is striking agreement between the phase and relative amplitudes of the sections, the yoyo and the barotropic v velocity. We conclude that the variations in depth and thickness (separation) of upper ocean density surfaces observed spatially along the sections may be explained primarily by tidal (temporal) variations, not by spatial variations.

An exception is the doming of the σ_0 = 26.15 kg m^{-3} isopycnal over the crest of Melville Bank during the second survey (Fig. 7a). This doming shows as a spike in Fig. 9 (just before 343/00) so is unlikely to be

tidal. Dimensional analysis indicated the possibility of a Taylor column over Melville Bank, but the currents throughout the water column were generally west to southwest. There was no evidence of recirculation around the seamount. The doming of the σ_0 = 26.15 kg m^{-3} isopycnal over the crest of the seamount is, therefore, perhaps the result of tidal rectification, which we consider further in section 5.2.

Isopycnal doming due to tides or tidal rectification can bring deeper, nutrient richer water into the euphotic zone and may create localised regions of high density stratification, that in turn may stabilise the water column helping to promote productivity (White et al., 2007). Weakly increased nutrient concentrations were observed over the seamount crest during the second section, but these were counter-balanced by the first section when low nutrient water was drawn down strongly. The fluorescent layer showed the same structure, with fluorescence extending deeper into the water column where the isopycnals were depressed and having shallower extent where the isopycnals were elevated. Thus over the seamount crest, fluorescence was confined to the upper 40 m in the second section, whereas on the first section fluorescence was observed all the way to the seabed at 100m. We conclude that the alternating deep and shallow fluorescence is not related to nutrient rich water from below, but to productivity in the euphotic zone alternately deepened and shallowed by vertical tidal motions.

The fluorescent layer is likely to be associated with biota that provide food for sessile organisms, thus the tidal cycle is likely to provide periodic bounty and famine at the seamount crest. Periodically there may be enrichment or depletion of nutrients and food. Thus vertical motions driven by tides can bring deeper water to the seamount crest while depletion of nutrients and increased availability of food is likely in the other half of the tidal cycle.

In summary, two nearly perpendicular CTD sections across Melville Bank revealed opposing conditions over the shallowest part, with warm water on the first section and cold water on the second section. Comparisons with the Egbert tidal model suggest that the variations are temporal (tidal) rather than spatial. A spike in isopycnal depth over the crest of the seamount is too extreme to be tidal. Together with local current variations the spike is consistent (by comparison with model results from Fieberling Seamount, section 5.2) with tidal rectification driving anticyclonic currents round the peak of the seamount. The fluorescent layer was strongly influenced by the circulation and it seems reasonable to assume that other fauna and flora were similarly affected.

4.5 Coral Seamount

Coral Seamount was located at 41° 25’S, 42° 51’E on the eastern side of the Discovery II Fracture Zone (Fig. 1a). Upper ocean water was subantarctic (Fig. 3) with mean temperature and salinity of 10.01°C and 34.56 in the upper 200m. The shallowest point of the seamount was roughly 100 m below the sea surface while the CTD yoyo was worked on the southwestern corner of the summit plateau in 425 m of water, above the steep drop off into the fracture zone (Fig. 1f). Sea surface height showed weak eastward advection of about 10-20 cm s^{-1} (Fig. 2), while shipboard currents during the survey showed variable flow from 0 to 50 cm s^{-1} with a generally eastward orientation.

The survey took place during spring tides and tidal effects were visible throughout the water column (Fig. 10). The 24-h CTD yoyo profiles showed the passage of two large-amplitude (150 m peak to trough)

semi-diurnal internal waves. Velocity measurements showed rapid changes in strength and direction with currents intensified during the passage of troughs and the direction rotating rapidly during the passage of wave crests. The effects of the tide extended up to the sea surface, where the fluorescence layer (Fig. 10f) was pushed upwards by the crest of the internal waves, lifting the base of the layer from about 100 m to less than 40 m depth. The thermocline was displaced vertically by over 150 m but asymmetrically. Internal wave crests were associated with steep peaks in properties, while the wave troughs were longer lasting with more gradual changes in depths of isolines. Asymmetry in displacement results from the presence of higher frequency waves, characteristic of non-linear tides in shallow waters (LeBlond and Mysak, 1981; Park et al., 2008).

The coldest water (6°C, 400 m) appeared at the seabed at about 3 and 16 hours into the CTD yoyo (Fig. 10a) 1-2 hours before the shallow crests (9°C, 100 m) at 5 and 17 hours. Thus phase velocity is propagating up, so energy is propagating down. This is still consistent with generation at the seabed because 400 m is deeper than the plateau (200-300 m, Fig. 1f), the depth at which internal waves are most likely to be generated.

The CTD section showed the salinity minimum of AAIW to be centred at 700 m depth to the north of the seamount and 600 m to the south (Fig. 11). At about 700 - 800 m there was pinching of isopycnals on the north side with shallower isopycnals near horizontal or sloping downwards to the south above this and sloping weakly upwards deeper than 800 m. In contrast, to the south of the seamount, the isopycnals sloped upwards to the south at all depths. The effect (assuming the isopycnal depth variations were spatial, not temporal) was to create a bowl shaped distribution of density in the upper layer, implying weak anticyclonic circulation around the seamount, but eastward flow below about 800 m.

The depth of the isopycnal σ_0 = 26.7 kg m^{-3} was plotted against time for the CTD section and yoyo and compared with the Egbert modelled barotropic tide (Fig. 9b). As at Melville, there is good agreement in both amplitude and phase between isopycnal displacements when connected by the model. We conclude that vertical displacements on the section are consistent with internal tidal oscillations. When the results were extended northwards along the transect towards Melville Bank (Fig. 9b), the isopycnals descended abruptly in the Subtropical and Agulhas Fronts, as required for geostrophic balance in the strong eastward flow of the Agulhas Return Current (Pollard and Read, 2015).

The t/s properties showed a sub-surface salinity minimum, with traces of a temperature minimum in the top 100m (Fig. 3, ‘A’). At the base of the fairly well mixed surface layer, strong stratification marked the transition to a salinity maximum of 34.7 - 34.8 associated with a temperature maximum (Fig. 3, ‘B’). At about 250m an inflexion in the t/s curve marked interleaving and small-scale minima and maxima in temperature and salinity (more pronounced in oxygen) (Fig. 3 ‘C’). The depth of 250 m was just below the summit of the seamount, although still shallower than the plateau (Fig. 1f). CTD profiles worked across the seamount showed a north-south gradient in isolines both above the seamount and deeper in the water column (Fig. 11). Interleaving and vertical maxima and minima in properties are evidence of strong stirring and mixing in the water column. There was no evidence of a Taylor Column, nor of tidal

rectification such as observed at Melville Bank. We look more closely at the mixing and water mass modification to try to understand the processes operating.

The vertical t/s profile of central water is usually a slight curve formed by double diffusion and defined by a density ratio (Read and Pollard, 1993; Schmitt, 1981). Such a relationship was observed at the subtropical seamounts (Fig. 3). However at Coral Seamount, the t/s profiles were not curved but formed straight line segments. This is particularly the case between the salinity maximum at about 100 m depth (Fig. 3, 'B') and the inflexion point at 250m ('C') and below the inflexion point ('C-D'). Curved t/s lines indicate diffusive mixing, while straight lines indicate direct mixing between water masses. The segment 'C-B' points to the end member STSW and the segment 'C-D' points to AAIW, however the water at point 'C' is up to 0.1 salinity units fresher than the SICW that fills the water column at this depth at the other seamounts (Fig. 3). This suggests fresh water input at the inflexion point.

The oxygen maximum just above 'C' (not shown), the low salinity indicative of surface waters and the weak stratification above that level (26.7 – 26.8 kg m^{-3}, Fig. 10c) suggest that 'C' marks the base of the mixed layer at the end of the preceding winter. The strong westerly winds that prevail in the "roaring forties" result in a northward Ekman flux that pushes the fresh surface water northwards, forcing it to subduct beneath lighter subtropical thermocline water (SICW, with temperature and salinity maxima) that lies to the north, 'B'. Thus the subantarctic surface water sinks beneath warmer subtropical water. The fresh subantarctic surface water 'A' overlying SICW 'B' has also been driven north by Ekman flux. Spring warming forms a shallow surface mixed layer above the winter surface water 'A'. In practice, alternating periods of strong wind and sunshine result in the interleaving which is apparent in Fig. 3.

Seasonal heating and northward flux, subduction and interleaving happen on large zonal and meridional scales dependent on the wind and surface forcing. They are unlikely to be influenced by the presence of seamounts. However, the interleaving at C is focussed at the depth of and just below the crest of the seamount at about 250 m depth, therefore it seems likely that the interaction of the currents, current shear and tides with the topography leads to enhanced mixing.

In summary, Coral Seamount was situated in the Subantarctic Zone close to the Subantarctic Front. Interleaving and water mass structure indicated strong mixing over the crest and upper part of the seamount. The fluorescence layer extended down to 100 m during troughs in the internal tides, reaching the seabed at the shallowest point of the plateau. Strong internal tides may also initiate the mixing. The t/s curve provides evidence for northward Ekman flux of fresh subantarctic surface water.

4.6 Walter Seamount

The seamount at 31° 37'S, 42° 49'E, northwest of Walter's Shoals on the Madagascar Ridge, was a low eminence of nearly circular plan (Fig. 1b). Satellite derived bathymetry (Fig. 1a) (Smith and Sandwell, 1997) suggested that the seamount shallowed to between 600-800 m depth, however swath bathymetry data collected during the cruise revealed a dome nowhere shallower than 1300 m (Fig. 1b). Altimetric sea surface height (Fig. 2) showed the seamount to be situated between two eddies. The eddy to the north consisted of lighter water circulating anticyclonically while the denser eddy to the south rotated cyclonically (Pollard and Read, 2015), hence flow past the seamount was eastwards. Near-

surface currents reached 70 - 80 cm s^{-1} during the first acoustic survey and were reduced to about 20 - 40 cm s^{-1} during the second. Mean temperature and salinity of the top 200 m averaged 18.30°C and 35.57 respectively (Fig. 3)

Weak variability in both CTD and yoyo data resulted primarily from basin scale circulation and there was little evidence of seamount influence. Horizontal gradients across the CTD section were associated with the eddy structure. In the bottom 100 m an increase in temperature and density across the crest of the seamount relative to background properties may have resulted from local topographic effects, but the difference was less than 0.2°C and 0.02 kg m^{-3}. The CTD yoyo, worked at the shallowest point of the dome, showed a cyclical variability in bottom properties that propagated up through the water column to about 800 m over a roughly semi-diurnal period, but at the seabed the change in temperature and density from the surface was less than 0.5°C and 0.05 kg m^{-3}.

We conclude that the presence of the seamount may influence the dynamics of the water column but the evidence is minimal and the major influence comes from mean and mesoscale circulation.

5. Discussion

In order to investigate the physical oceanography at the 6 seamounts, it is useful to calculate several non-dimensional parameters for each seamount (Table 1). The mean velocity U was calculated from the ADCP data and the mean stratification. N (the Brunt-Väisälä frequency), was calculated from the CTD data during the 24-h yoyos. The geometry of the seamounts, as given by L (the horizontal length scale of the seamount), H (the depth of the water column away from the seamount) and h_0 (the height of the seamount), was estimated from the swath bathymetry.

The Rossby number, Ro = U/fL, compares the inertial and rotational terms of the equation of motion, describing the importance of the earth's rotation in determining the governing dynamics over the seamount. U and L are defined above and f is the Coriolis parameter. For each seamount, small Ro (Table 1) shows that the earth's rotation is hugely important to the dynamics of flow near seamounts

The Burger number, B=NH/fL, expresses the importance of local stratification (Huppert, 1975). B < 1 indicates nearly unstratified conditions, B > 1 indicates that the water is stratified. From Table 1 it is clear that the water column near all seamounts is stratified, but at Sapmer the stratification is significantly weaker than at all other seamounts (Pollard and Read, 2015).

5.1 Taylor Caps

In certain circumstances, water can be trapped over the crest of a seamount, forming what is known as a Taylor column (Taylor, 1917) or Taylor cap (Chapman and Haidvogel, 1992; Lavelle and Mohn, 2010), depending on whether the water is unstratified or stratified (our situation). [The term Taylor cone is sometimes found but should be reserved for GI Taylor's contribution to electrical field theory (Taylor, 1964)]. A Taylor cap is an isolated region of water trapped above the topography (Hogg, 1973) which has been hypothesised to influence the distribution of biota by retention of plankton over the summit (White et al., 2007). Several seamounts were observed during the CTD transects to have anomalously cold water over the crest relative to the background property fields. This is a typical feature of Taylor

caps but can also occur through tidal rectification or simply vertical motion associated with internal tides. We can assess whether the formation of a Taylor cap is possible by calculating a blocking parameter ($Bl = \alpha/Ro$), where $\alpha = h_0/H$ is the scaled height of the seamount. If $Bl > 2$ then a Taylor cap can form (Chapman and Haidvogel, 1992; White et al., 2007). All six seamounts have high blocking factors, the lowest being the two deep seamounts, Middle of What and Walter ($Bl = 5$). The three seamounts with the highest blocking factors, Coral, Melville and Atlantis ($Bl = 14, 12, 12$), were those that penetrated high into the water column hence presented a greater obstacle to the flow.

Thus the geometry and stratification at each seamount are conducive to Taylor cap formation. To investigate whether or not Taylor caps were present, the ADCP grids were inspected for signs of circular flow. Only Atlantis Bank and Sapmer Seamount showed any hint of this. All other seamounts exhibited nearly linear flow throughout the water column.

Atlantis Bank had a nearly closed circulation in the surface layer, but with depth this transformed into a linear, cross-seamount flow. For a Taylor cap, the opposite is required, namely closed circulation close to the seamount crest, decreasing towards the surface. Thus the nearly-closed circulation above Atlantis was not produced by a Taylor cap.

ADCP data collected at Sapmer Seamount showed no convincing recirculation. The water column at Sapmer was very weakly stratified (section 4.2). Density showed only a hint of isopycnal doming, but dissolved oxygen (not shown), which had strong gradients, showed significant doming over the seamount. The implication is that there may have been a Taylor cap above Sapmer Seamount, but the evidence is weak.

Our conclusion is that, while in principle Taylor caps could exist over all seamounts, in practice the relatively large currents associated with mesoscale eddies prevented their formation, or swept away any incipient Taylor caps before they could become established.

5.2 Rectified flow

We only found one instance of vertical displacement of an isotherm that could not be explained as tidal variation (at Melville Bank, section 4.4). The dense (and cold) anomaly over the crest of Melville Bank had an elevation of about 71 m more than the tidal fit (Fig. 9) with a temperature anomaly of order 0.8°C. These anomalies are the same order of magnitude as found in a model (Lavelle, 2006) fitted to Fieberling Seamount, in which tidal flow was rectified to produce toroidal flow around the summit. Toroidal flow was not identified at Melville, but currents are hard to measure at sea, especially at the scale required. Also, the model describes conical seamounts (Lavelle, 2006; Lavelle et al., 2004) whereas Melville Bank was elongated west to east.

If rectified flow encircled the Bank, it would need to flow eastwards along the south side and westwards along the north side of the crest. An exception to the generally southwestward flow was the station at 38.478°S on the N-S section (Fig. 7a). The station was immediately south of the seamount crest (Fig. 1g) and showed a complete reversal of flow between 80 - 250 m, i.e., below the depth of the crest (90 m). Here the current was about 24 cm s^{-1} eastwards along the south side of the ridge crest. At the same

depth there was an uplift in the isopycnals. The scale and strength of the feature was similar to that found associated with tidal rectification at Fieberling Seamount (Lavelle, 2006)

For flow to continue anticyclonically around the crest of the seamount, it must follow the contours across the E-W section at about 46.767°E. Unfortunately no CTD was worked at that point, the stations being located on the crest of the ridge and on the shoulder further down the ridge to the east. Similarly, the station to the north was located too far down the seamount slope to observe any reverse flow. So despite station spacing of 1-2 km, it was insufficient to map the local circulation. However, such evidence as was collected was consistent with tidally rectified currents around the seamount.

5.3 Enhanced internal tides near seamounts

A clear semi-diurnal tidal signal was apparent in the 24-h CTD yoyo at several seamounts (e.g. Figs 4, 5 and 10), sometimes dominating temporal variability (Fig. 10). Internal tides are initiated by the interaction of the barotropic tide (Egbert and Erofeeva, 2002) with the bathymetry of the seamount (Baines, 2007). Enhancement of the internal tide by and near a seamount has several consequences. Enhanced tides will alias the spatial variations of the short CTD sections, may drive tidal rectification and may result in enhanced mixing.

Time constraints (less than 12 hours survey time) only allowed for short (less than 10 km) CTD sections across the summit of each seamount. We have described these in spatial terms but were aware that the strong semi-diurnal tide might swamp any spatial signal. We were able to examine this possibility at Melville and Coral by plotting the phase of a component of the barotropic tide against time and comparing it with the depth of a density surface for all CTDs in the vicinity, also plotted against time, whether the CTDs were part of the 24-h CTD yoyo, part of a short section, or indeed part of a long section. The results (Fig. 9) showed clearly that the depth variations of the short section CTDs were in phase with tidal variations seen in the 24-h CTD yoyo, so are most likely to be aliased temporal variations rather than spatial variations. Thus all spatial variations along the short CTD sections must be viewed with caution. However, for the long sections (Fig. 9b), spatial variations dominate tidal variations for scales greater than about 30 km.

Evidence that internal tides are generated near the crests of seamounts comes from examination of internal tidal propagation. At Sapmer and Melville, tidal energy was found to be propagating up from the seabed. At Coral, at depths below the crest, tidal energy was found to be propagating downwards.

5.4 Mixing

Enhanced tidal energy near the seamount crests leads to enhanced shear, which reduces the Richardson number, the ratio of stratification to shear. If the stratification is weak enough, such that Ri drops below 0.25, then the shear leads to mixing. Evidence for low Ri was found at Sapmer and Middle of What, both of which were affected, at the time of the survey, by a deep anticyclonic eddy and hence weak stratification, particularly so at Sapmer.

Relatively weak stratification at the depth of the seamount crest, even when it is well below the depth of the seasonal mixed layer, may identify the residual mixed layer from deep winter mixing the previous

winter. This was particularly the case at Coral, where weakly stratified water below 100 m down to the depth of the seamount crest (200 m) was shown to have the characteristics of winter water.

6. Conclusions

Mean currents in the vicinity of each seamount were dominated by mesoscale eddies, with mean speeds of 15-25 cm s^{-1} (Table 1). Melville Bank, Coral and Middle of What Seamounts were also influenced by the strong flow of the Agulhas Return Current. From the very weak evidence for Taylor caps and rectified currents, we infer that the mean currents are large enough to largely prevent the formation of circulation trapped to each seamount.

The dominant oscillatory currents were tidal, on which the seamounts had a much larger influence. From the good correlation between the barotropic tides and internal tides at Coral and Melville, we deduce that the internal tides are initiated by interaction of the barotropic tide and the seamounts. This occurs particularly near the crest of each seamount, resulting in energy propagating downwards below the summit of a seamount (Coral) and upwards above the summit of other seamounts (Sapmer and Melville). Internal tides caused vertical displacements of isopycnals of up to 200 m peak to trough. The depth of the mixed layer and fluorescence layer also varied considerably with the tides (e.g. Fig. 10d), exposing the shallower seamount summits (Melville, Coral) to the euphotic zone each tidal cycle. Tidal temperature changes extended to the deeper seamount summits with temperature variability across the tidal cycle varying from 0.5°C (Walter) through 0.8°C (Sapmer, Melville) and 1°C (Atlantis, Middle of What) to 3°C (Coral).

The enhanced current shear of the internal tides was sufficient to overcome relatively weak stratification near the summits of several seamounts, resulting in low Richardson numbers and hence mixing. At Sapmer and Middle of What, weak stratification resulted from the presence of an anticyclonic mesoscale eddy. At Coral, weak stratification was associated with remnant winter water, i.e. the remains of a deep winter mixed layer. Thus, while the enhanced tidal shear was a consequence of the presence of a seamount, the weak stratification was not.

The strong vertical motions of the internal tides aliased the spatial variations shown in short sections across each seamount summit. Only when spatial separation between CTD stations increased to 30 km (Fig. 9b) did geostrophic isopycnal slopes dominate internal tidal temporal variations.

Acknowledgements

The authors would like to thank the officers, crew and scientists of the RV Dr Fridtjof Nansen cruise 2009 410 without whose help these data would not have been collected. This work was supported by the NERC large scale observing programme.

Figures

Fig. 1a. Bathymetry of the Southwest Indian Ocean. Contours at 500, 1000, 2000, 3000, 4000, 5000 m, shading shallower than 1000 m and deeper than 4000 m. Walter - Unnamed seamount off Walter's Shoals, FZ - Fracture Zone. CTD locations shown by filled circles. Topography of individual seamounts: b) Walter Seamount, c) Atlantis Bank, d) Middle of What Seamount, e) Sapmer Seamount, f) Coral

Seamount, g) Melville Bank. Bathymetry contoured every 100 m with bold contours every 500 m, except Walter and Middle of What Seamounts, which are contoured every 50 m with bold lines every 200 m. Stars indicate CTD positions with multiple CTDs marking the location of the yoyo.

Fig. 2. Colours show Modis Aqua chlorophyll a 7 day composite 11 - 18 December 2009, note the non-linear colour scale. Contours show AVISO sea surface height from merged absolute dynamic topography for 16 - 24 December 2009, contour intervals 10 cm with bold lines at 0 and every 50 cm. The Agulhas Return Current is shown by the band of closely spaced contours on the northern edge of the high chlorophyll a zone. CTD station positions are indicated by asterisks with repeated stations marking seamount locations. The cruise track is indicated by dashed line.

Fig. 3. Potential temperature / salinity of all CTD profiles from the RV Dr Fridtjof Nansen cruise 410 2009. Profiles are colour coded by location. TSW - Tropical Surface Water, STSW - Subtropical Surface Water, SICW - South Indian Central Water, SASW – Subantarctic Surface Water, AAIW - Antarctic Intermediate Water. See text for explanation of letters A, B, C and D.

Fig. 4. Density (referenced to the surface) across a) Atlantis Seamount and b) over a 24-hour period, c) east and north velocities over the top 300 m of the water column. Short tick marks on the x axis of figures a and b indicate positions of CTD profiles. Velocity x and y axes are east and north and do not show vertical movement. Time in hours past the start time of 17 Nov 2009, 15:00 (day 321).

Fig. 5. a) Potential temperature θ ($0.05°$contours, b) salinity (0.005 contours), c) density σ_0 (0.01 kg m^{-3} contours), d) Brünt-Väisäla frequency N (cycles per hour) and e) Richardson Number Ri at Sapmer Seamount during a 24-hour period. Time in hours past the start time of 22 Nov 2009, 15:00 (day 326).

Fig. 6. Lowered ADCP velocities across Middle of What Seamount superimposed on density σ_0. Velocity x and y axes are east and north respectively and do not show vertical motion. Small tick marks on the x axis indicate positions of CTD profiles. Dark grey bars mark areas where there is a 50% probability of Richardson numbers Ri < 1, likely to enhance internal mixing.

Fig. 7. a) north-south and b) west-east density contours across Melville Bank. Current vectors are from vessel-mounted ADCP measurements, x and y axes are east and north velocity. Short tick marks on the x axes indicate CTD station position.

Fig. 8. Melville Bank a) potential temperature, b) salinity, c) density and d) velocity measured over 24 hours starting at day 343/0955, 9 December 2009 at Melville Bank. Velocity x and y are east and north coordinates.

Fig. 9. Isopycnal pressure of (a) 26.2 kg m^{-3} at Melville Bank and (b) 26.7 m^{-3} at Coral Seamount against time are compared with predicted north velocity (v) from the Egbert tidal model (Egbert and Erofeeva, 2002), dashed line. Individual CTDs are marked +. The CTDs (yoyo and sections) at each site were all within a circle of 5 km radius. The start of the CTD transect from Coral to Melville (station spacing 32 km) is shown dashed in b), demonstrating that spatial variations dominate tidal variations for scales > 30 km.

A short section of isopycnal 26.15 kg m^{-3} at Melville shows the anomalously shallow (relative to the tide) dense cap (the spike) over the seamount.

Fig. 10. Coral Seamount a) potential temperature (0.5°C contours), b) salinity (0.05 contours), c) density σ_0 (0.05 kg m^{-3} contours), d) fluorescence (monotonic grey shades) and e) velocity measurements over a 24-h period (x and y axes are east and north coordinates). Time is shown in hours past the start time, day 337/0258, 3 December 2009.

Fig. 11. CTD section across Coral Seamount, a) potential temperature, b) salinity and c) density referenced to the surface. Short tick marks on the x axes indicate CTD positions.

References

Baines, P.G., 2007. Internal tide generation by seamounts. Deep Sea Research I 54, 1486-1508, doi:10.1016/j.dsr.2007.05.009.

Belkin, I.M., Gordon, A.L., 1996. Southern Ocean fronts from the Greenwich Meridian to Tasmania. J. Geophys. Res. 101, 3675-3696, doi:10.1029/95JC02750.

Chapman, D.C., Haidvogel, D.B., 1992. Formation of Taylor caps over a tall isolated seamount in a stratified ocean. Geophy. Astrophys. Fluid Dyn. 64, 31-65, doi:10.1080/03091929208228084.

Clark, M.R., Rowden, A.A., Schlacher, T., Williams, A., Consalvey, M., Stocks, K.I., Rogers, A.D., O'Hara, T.D., White, M., Shank, T.M., 2010. The ecology of seamounts: structure, function, and human impacts. Ann. Rev. Mar. Sci. 2, 253-278, doi:10.1146/annurev-marine-120308-081109.

Dick, H., 1998. Indian Ocean's Atlantis Bank yields deep-earth insight. Oceanus 41, 29-32.

Egbert, G.D., Erofeeva, S.Y., 2002. Efficient Inverse Modeling of Barotropic Ocean Tides. J. Atmos. & Oceanic Tech. 19, 183-204, doi:10.1175/1520-0426(2002)019<0183:EIMOBO>2.0.CO;2.

Egbert, G.D., Ray, R.D., 2001. Estimates of M2 tidal energy dissipation from TOPEX/Poseidon altimeter data. J. Geophys. Res. 106, 22475-22502, doi:10.1029/2000JC000699.

Garrett, C., 2003. Internal tides and ocean mixing. Science 301, 1858-1859, doi:10.1126/science.1090002

Genin, A., 2004. Bio-physical coupling in the formation of zooplankton and fish aggregations over abrupt topographies. J. Mar. Sys. 50, 3-20, doi:10.1016/J.Marsys.2003.10.008.

Genin, A., Dower, J.F., 2007. Seamount plankton dynamics, in: Pitcher, P., Morato, T., Hart, P., Clark, M., Haggan, N., Santos, R. (Eds.), Seamounts: ecology, fisheries and conservation, Fish and Aquatic Resources Series 12, Blackwell Publishing, Oxford, UK, pp. 85-100.

Gill, A.E., 1982. Atmosphere-ocean dynamics. Academic press, 662 pp.

Hogg, N.G., 1973. On the stratified Taylor column. J. Fluid Mech. 58, 517-537, doi:10.1017/S0022112073002302

Huppert, H.E., 1975. Some remarks on the initiation of inertial Taylor columns. J. Fluid Mech. 67, 397-412, doi:10.1017/S0022112075000377.

Klymak, J.M., Moum, J.N., 2003. Internal solitary waves of elevation advancing on a shoaling shelf. Geophys. Res. Lett. 30, doi:10.1029/2003GL017706.

Lavelle, J., 2006. Flow, hydrography, turbulent mixing, and dissipation at Fieberling Guyot examined with a primitive equation model. J. Geophys. Res. 111, doi:10.1029/2005JC003224.

Lavelle, J., Lozovatsky, I., Smith, D., 2004. Tidally induced turbulent mixing at Irving Seamount—modeling and measurements. Geophys. Res. Lett. 31, doi:10.1029/2004GL019706.

Lavelle, J., Mohn, C., 2010. Motion, commotion, and biophysical connections at deep ocean seamounts. Oceanography 23, 90-103.

LeBlond, P.H., Mysak, L.A., 1981. Waves in the Ocean. Elsevier.

Park, Y.H., Fuda, J.L., Durand, I., Garabato, A.C.N., 2008. Internal tides and vertical mixing over the Kerguelen Plateau. Deep-Sea Res. II 55, 582-593, doi:10.1016/j.dsr2.2007.12.027.

Pollard, R.T., Read, J.F., 2015. Circulation, stratification and seamounts in the Southwest Indian Ocean. Deep-Sea Res. II this issue, doi:10.1016/j.dsr2.2015.02.018.

Read, J.F., Pollard, R.T., 1993. Structure and transport of the Antarctic Circumpolar Current and Agulhas Return Current at 40°E. J. Geophys. Res. 98, 12281-12295, doi:10.1029/93JC00436.

Rogers, A., 1994. The biology of seamounts. Adv. in Mar. Biol. 30, 305-350, doi:10.1016/S0065-2881(08)60065-6.

Rogers, A., Alvheim, O., Bemanaja, E., Benivary, D., Boersch-Supan, P., Bornman, T., Cedras, R., DuPlessis, N., Gotheil, S., Høines, A., Kemp, K., Kristiansen, J., Letessier, T., Mangar, V., Mazungula, N., Mørk, T., Pinet, P., Pollard, R.T., Read, J., Sonnekus, T., 2014. Pelagic communities of the South West Indian Ocean seamounts: R/V/ *Dr Fridtjof Nansen* cruise 2009-410. Deep-Sea Res. II this issue.

Rogers, A., Alvheim, O., Bemanaja, E., Benivary, D., Boersch-Supan, P., Bornman, T., Cedras, R., DuPlessis, N., Gotheil, S., Høines, A., Kemp, K., Kristiansen, J., Letessier, T., Mangar, V., Mazungula, N., Mørk, T., Pinet, P., Read, J., Sonnekus, T., 2009. "Dr. Fritjof Nansen" Southern Indian Ocean Seamounts (IUCN/UNDP/ASCLME/NERC/EAF Nansen Project 2009 Cruise 410) 12th November – 19th December. Gland, CH, International Union for Conservation of Nature, 12/2009, in: Secondary Rogers, A., Alvheim, O., Bemanaja, E., Benivary, D., Boersch-Supan, P., Bornman, T., Cedras, R., DuPlessis, N., Gotheil, S., Høines, A., Kemp, K., Kristiansen, J., Letessier, T., Mangar, V., Mazungula, N., Mørk, T., Pinet, P., Read, J., Sonnekus, T. (Eds.), Secondary "Dr. Fritjof Nansen" Southern Indian Ocean Seamounts (IUCN/UNDP/ASCLME/NERC/EAF Nansen Project 2009 Cruise 410) 12th November – 19th December. Gland, CH, International Union for Conservation of Nature, 12/2009, 188 pp.

Rowden, A.A., Dower, J.F., Schlacher, T.A., Consalvey, M., Clark, M.R., 2010. Paradigms in seamount ecology: fact, fiction and future. Mar. Ecol. 31, 226-241, doi:10.1111/j.1439-0485.2010.00400.x.

Schmitt, R.W., 1981. Form of the temperature-salinity relationship in the central water: evidence for double-diffusive mixing. J. Phys. Oceanogr. 11, 1015-1026, doi:10.1175/1520-0485(1981)011<1015:FOTTSR>2.0.CO;2.

Shank, T.M., 2010. Seamounts: deep-ocean laboratories of faunal connectivity, evolution, and endemism. Oceanography 23, doi:10.5670/oceanog.2010.65.

Smith, W.H., Sandwell, D.T., 1997. Global sea floor topography from satellite altimetry and ship depth soundings. Science 277, 1956-1962, doi:10.1126/science.277.5334.1956

Sparrow, M.D., Heywood, K.J., Brown, J., Stevens, D.P., 1996. Current structure of the south Indian Ocean. J. Geophys. Res. 101, 6377-6391, doi:10.1029/95JC03750.

Taylor, G.I., 1917. Motion of solids in fluids when the flow is not irrotational. Proc. Roy. Soc. London A93, 99-113, doi:10.1098/rspa.1917.0007.

Taylor, G.I., 1964. Disintegration of water droplets in an electric field. Proc. Roy. Soc. A A280, 383-397, doi:10.1098/rspa.1964.0151.

White, M., Bashmachnikov, I., Arístegui, J., Martins, A., 2007. Physical processes and seamount productivity, in: Pitcher, P., Morato, T., Hart, P., Clark, M., Haggan, N., Santos, R. (Eds.), Seamounts: ecology, fisheries and conservation, Fish and Aquatic Resources Series **12**, Blackwell Publishing, Oxford, pp. 65-84.

Table 1. Surveyed Seamounts

Seamount		Atlantis	Sapmer	Middle of What	Coral	Melville	Walter
latitude	°S	32.6-23.9	36.7-37.0	37.8-38.1	41.3-41.6	38.3-38.6	31.5-31.8
longitude	°E	57.1-57.5	51.9-52.3	50.2-50.6	42.7-43.1	46.5-46.9	42.6-43.1
mean latitude		32° 42' S	36° 51' S		41° 25' S	38° 28' S	31° 37' S
mean longitude		57° 16'E	52° 9' E		42° 51' E	42° 49' E	42° 49' E
minimum depth	m	750	350	1100	200	100	1250
date occupied	2009	17-19 Nov	22-24 Nov	25-27 Nov	2-4 Dev	7-10 Dec	12-13 Dec
day of year	2009	321-323	326-328	329-331	336-338	341-344	346-347
speed	cm/s	12.9	21.4	25.2	17.4	10.8	20.3
direction	degrees	60	90	74	84	61	80
height of seamount (h_0)	m	1650	1650	900	1800	2000	750
depth of water column (H)	m	2400	2000	2000	2000	2100	2000
alpha (α)	h_0/H	0.69	0.82	0.45	0.90	0.95	0.37
seamount width (L)	km	27.8	27.8	27.8	27.8	15.0	33.4
flow speed (U)	m/s	0.13	0.21	0.25	0.17	0.11	0.2
f ($2\omega\sin(lat)$)	10^{-5} rad/s	7.9	8.8	9.0	9.7	9.1	7.6
inertial period	hours	22.1	19.8	19.4	18.0	19.2	23.0
Rossby number (Ro)	U/(fL)	0.059	0.088	0.101	0.065	0.079	0.080
Blocking factor (Bl)	α/Ro	11.7	9.4	4.5	13.8	12.0	4.7
Brünt-Väisäla frequency (N)	rad/s	0.0044	0.0014	0.0028	0.0035	0.0030	0.0057
decay height (Hd)	fL/N	498	1737	891	767	458	446

Rossby radius of deformation (Lr)	(NH)/f	133.9	32.0	62.4	72.5	694.1	149.6
Burger number (B)	(NH)/ (fL)	4.82	1.15	2.25	2.61	4.63	4.49

Figure 1a

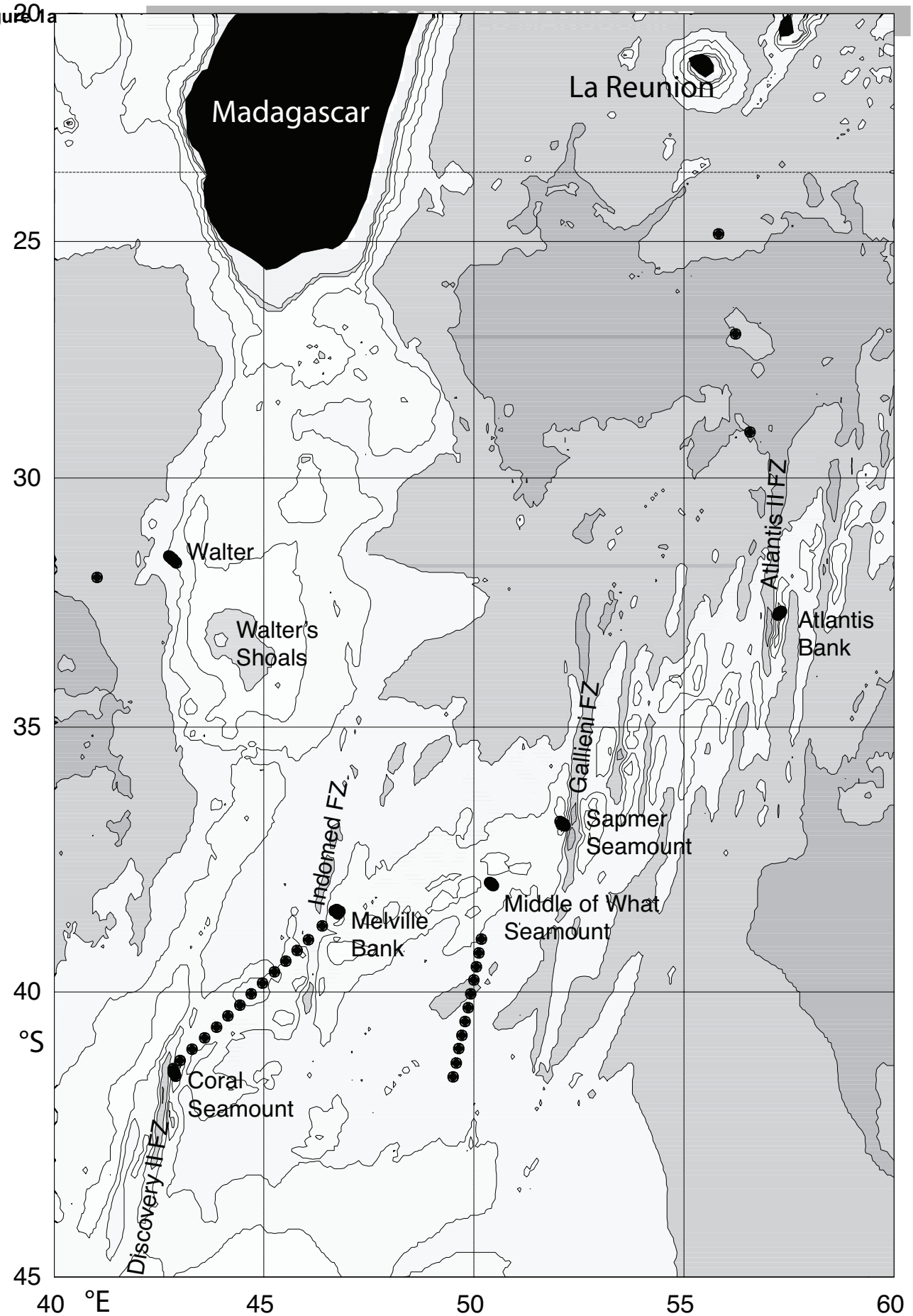

Fig. 1a. Bathymetry of the Southwest Indian Ocean. Contours at 500, 1000, 2000, 3000, 4000, 5000 m, shading shallower than 1000 m and deeper than 4000 m. Walter – Unnamed seamount off Walter's Shoals, FZ – Fracture Zone. CTD locations shown by filled circles.

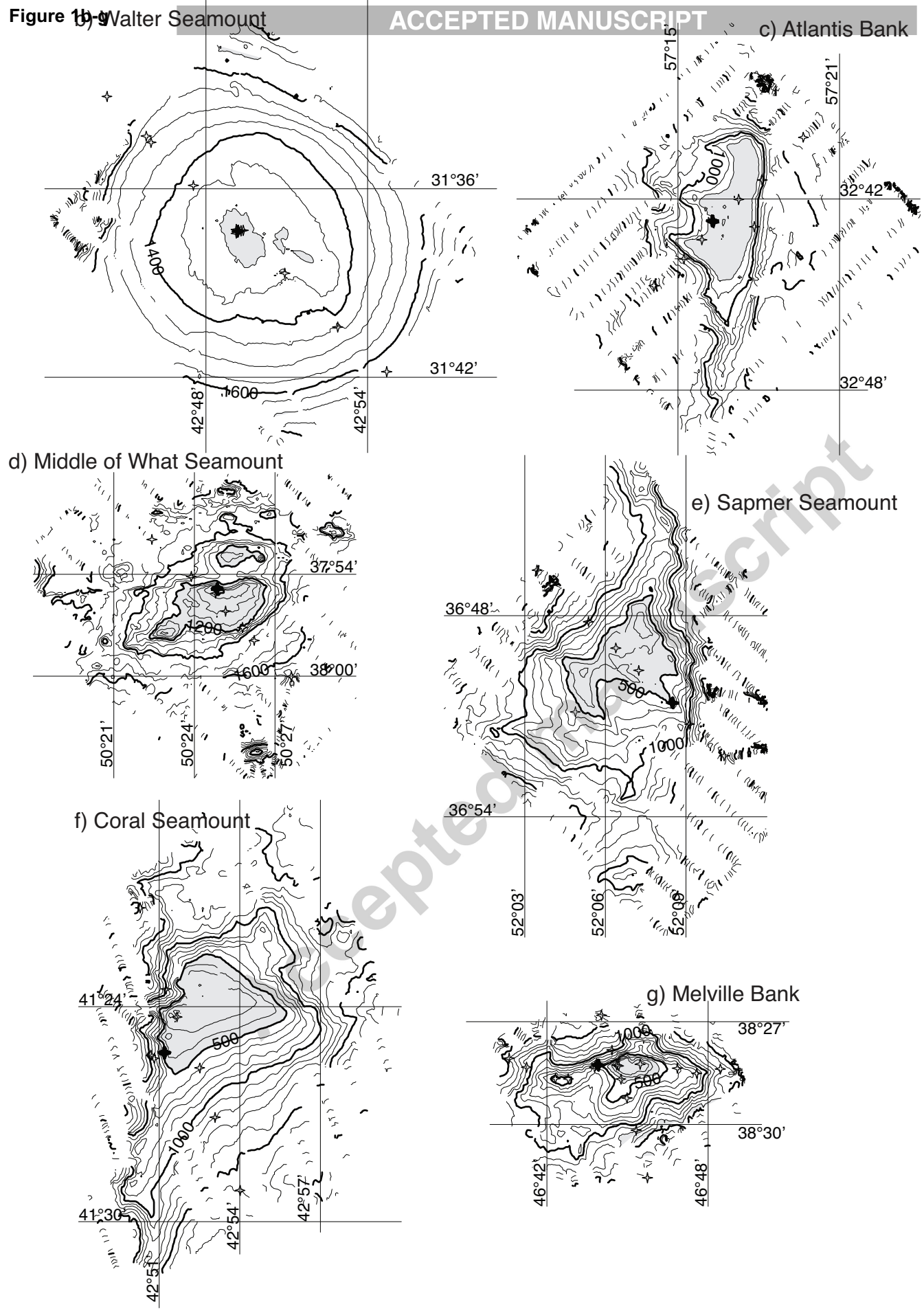

Fig. 1b-g - Topography of individual seamounts: b) Walter Seamount, c) Atlantis Bank, d) Middle of What Seamount, e) Sapmer Seamount, f) Coral Seamount, g) Melville Bank. Bathymetry contoured every 100 m with bold contours every 500 m, except Walter and Middle of What Seamounts, which are contoured every 50 m with bold lines every 200 m. Stars indicate CTD positions with multiple CTDs marking the location of the yoyo.

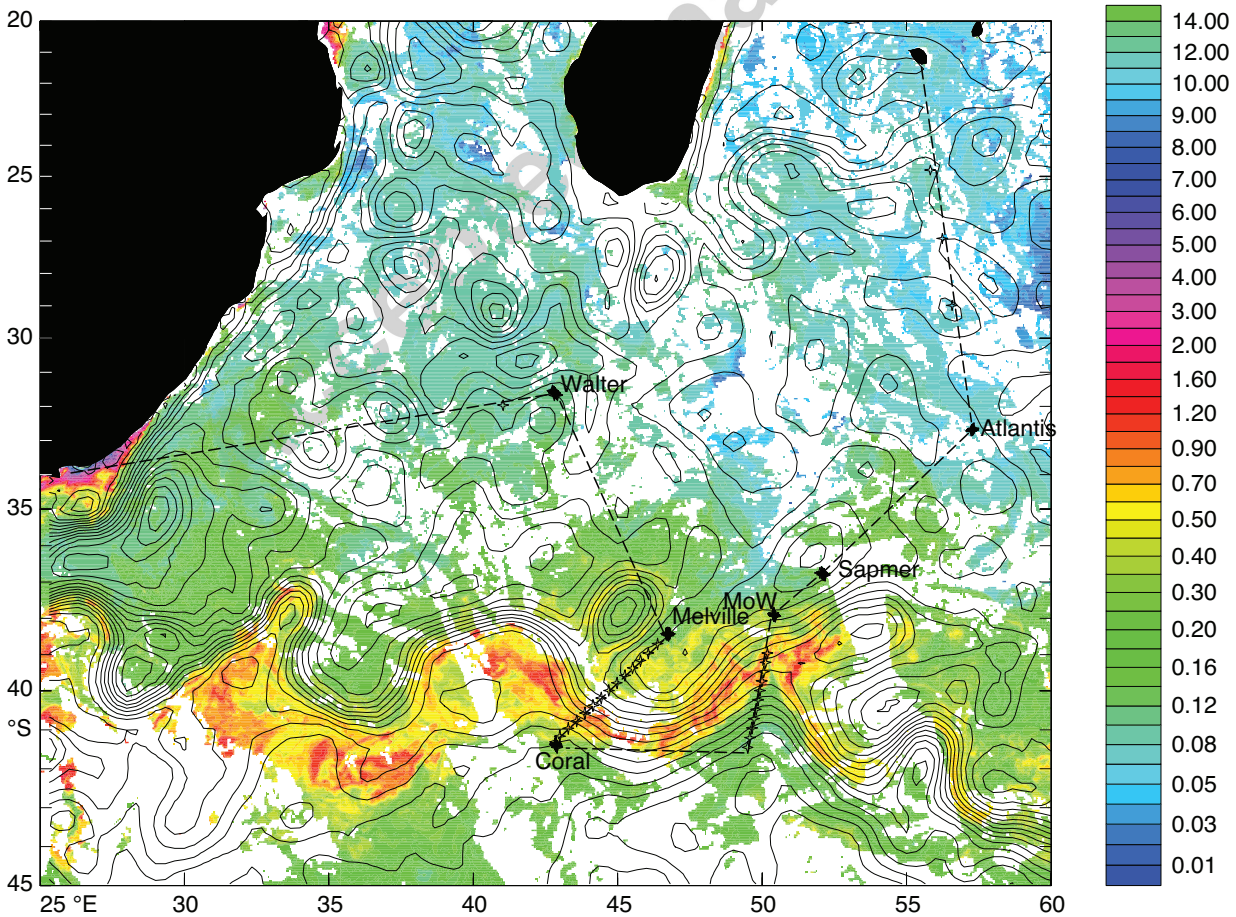

Fig. 2. Colours show Modis Aqua chlorophyll a 7 day composite 11 – 18 December 2009, note the non-linear colour scale. Contours show AVISO sea surface height from merged absolute dynamic topography for 16 – 24 December 2009, contour intervals 10 cm with bold lines at 0 and every 50 cm. The Agulhas Return Current is shown by the band of closely spaced contours on the northern edge of the high chlorophyll a zone. CTD station positions are indicated by asterisks with repeated stations marking seamount locations. The cruise track is indicated by dashed line.

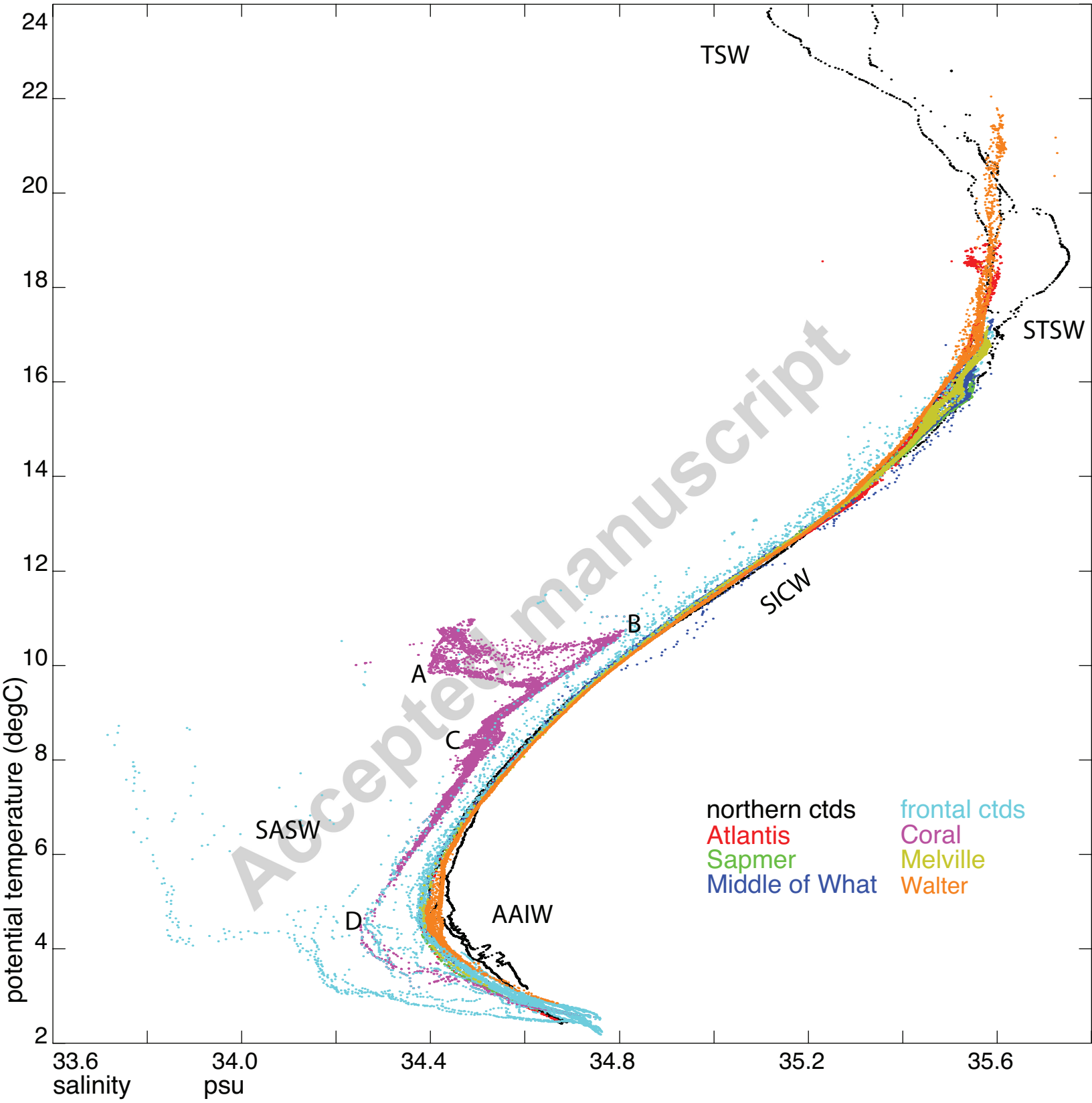

Figure 3. Potential temperature / salinity relationship of all CTD profiles from the RV Dr Fridtjof Nansen cruise 410 2009. Profiles are colour coded by location. TSW - Tropical Surface Water, STSW - Subtropical Surface Water, SICW - South Indian Central Water, SASW - Subantarctic Surface Water, AAIW - Antarctic Intermediate Water. See text for explanation of letters A, B, C and D.

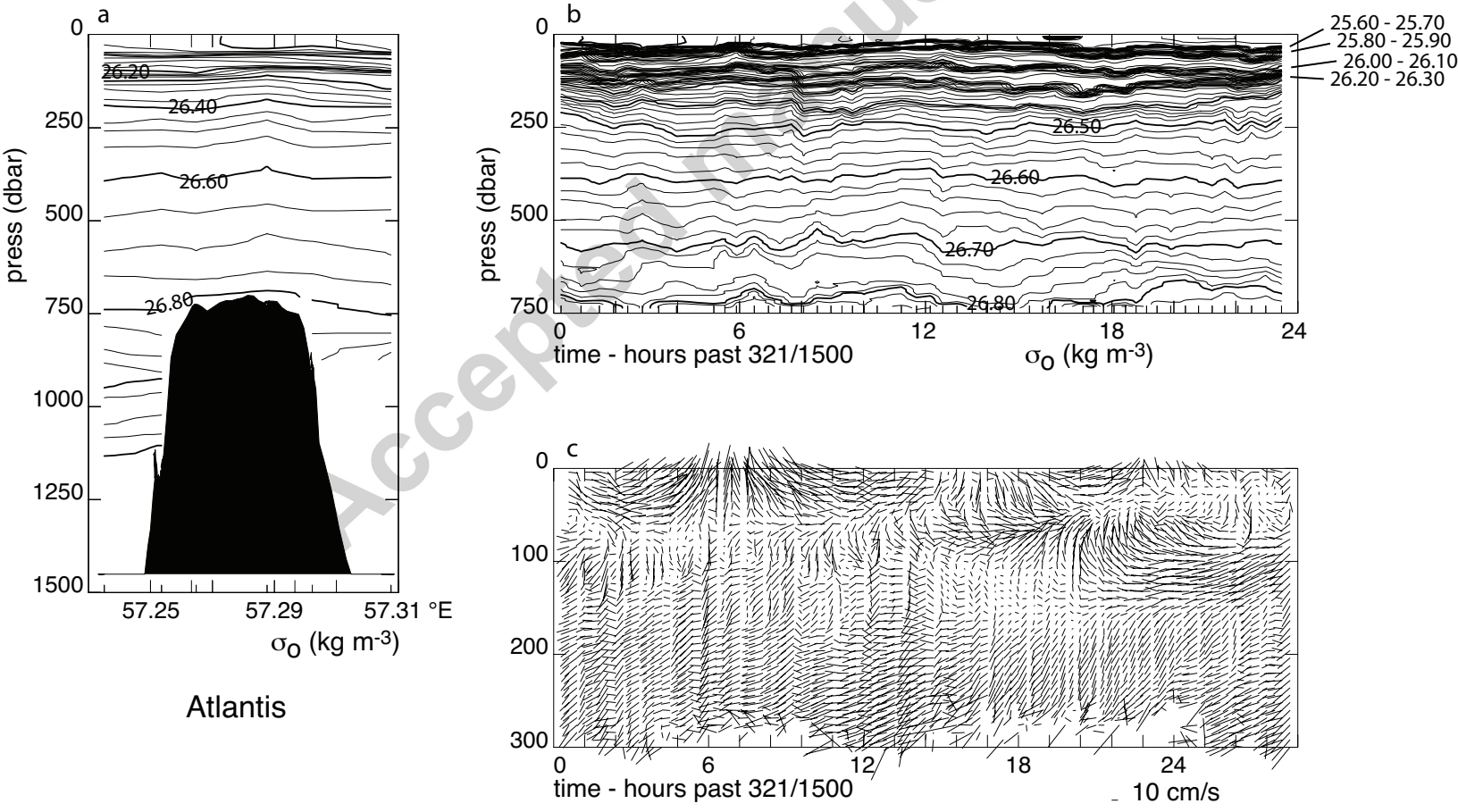

Fig. 4. Density (referenced to the surface) across a) Atlantis Seamount and b) over a 24-hour period, c) east and north velocities over the top 300 m of the water column. Short tick marks on the x axis of figures a and b indicate positions of CTD profiles. Velocity x and y axes are east and north and do not show vertical movement. Time in hours past the start time of 17 Nov 2009, 15:00 (day 321).

Figure 5

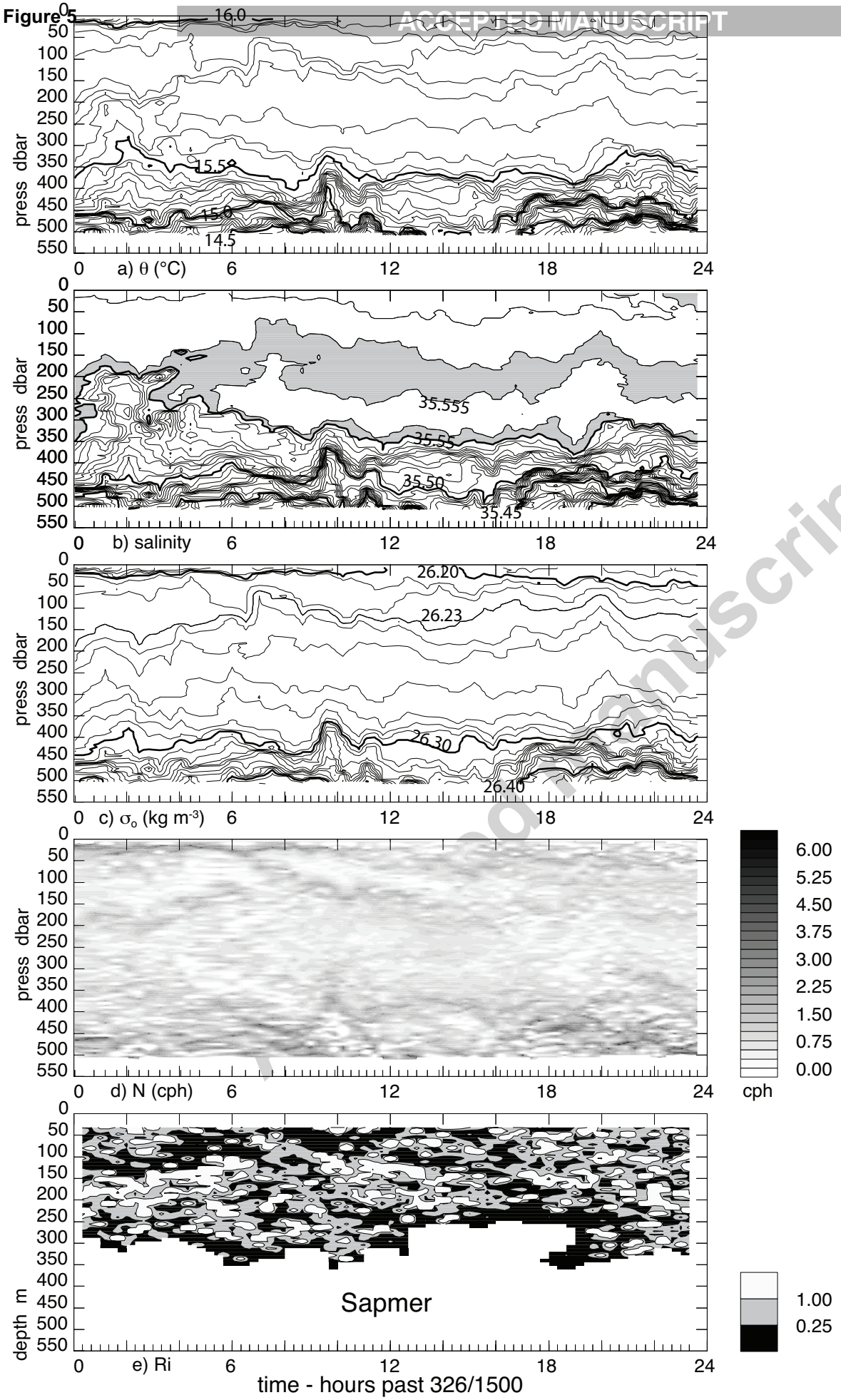

Fig. 5. a) Potential temperature θ (0.05° contours), b) salinity (0.005 contours), c) density σ_0 (0.01 kg m^{-3} contours), d) Brünt-Väisäla frequency N (cycles per hour) and e) Richardson Number Ri at Sapmer Seamount during a 24-hour period. Time in hours past the start time of 22 Nov 2009, 15:00 (day 326).

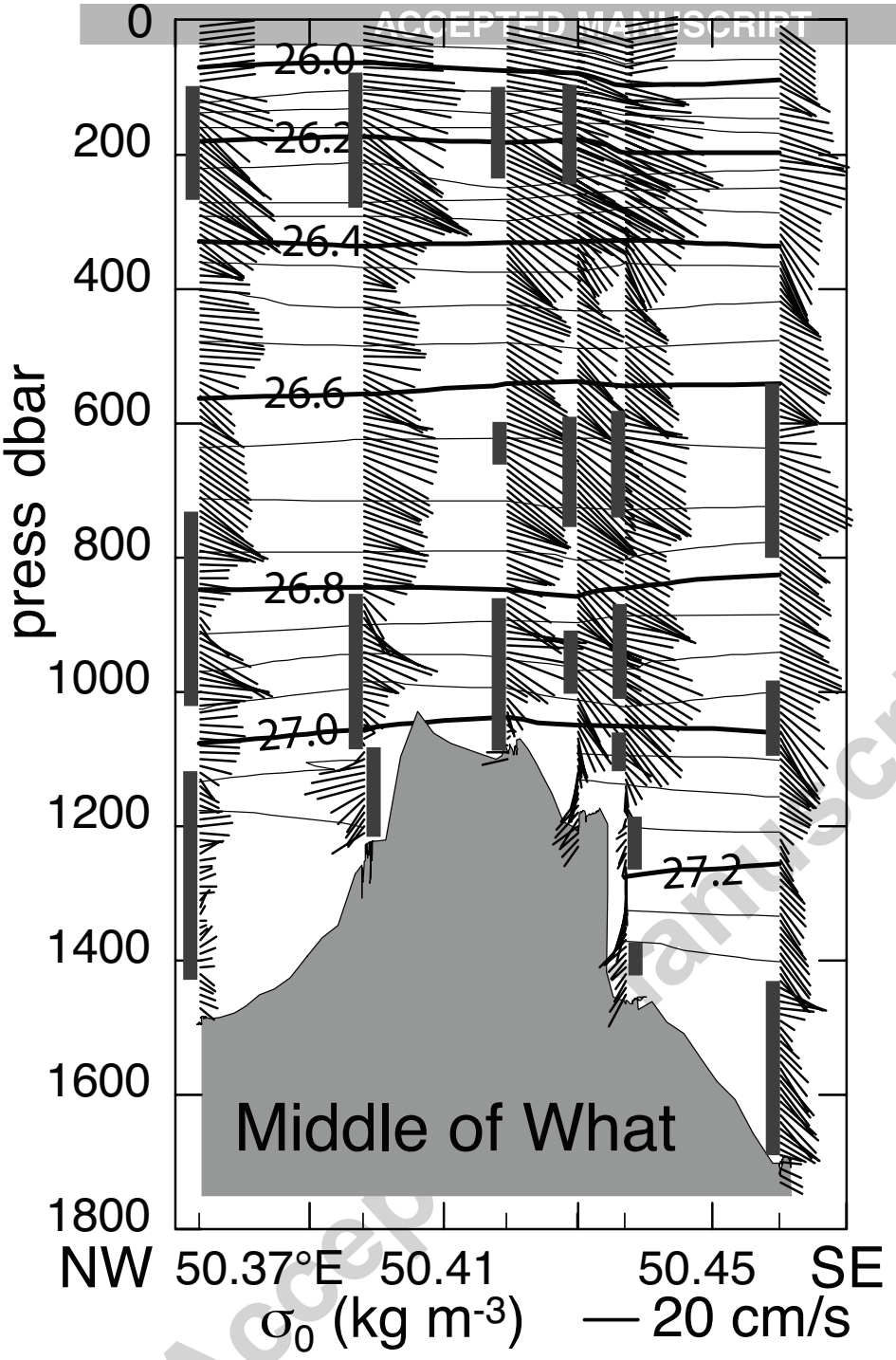

Fig. 6. Lowered ADCP velocities across Middle of What Seamount superimposed on density σ_0. Velocity x and y axes are east and north respectively and do not show vertical motion. Small tick marks on the x axis indicate positions of CTD profiles.. Dark grey bars mark areas where there is a 50% probability of Richardson numbers Ri < 1, likely to enhance internal mixing.

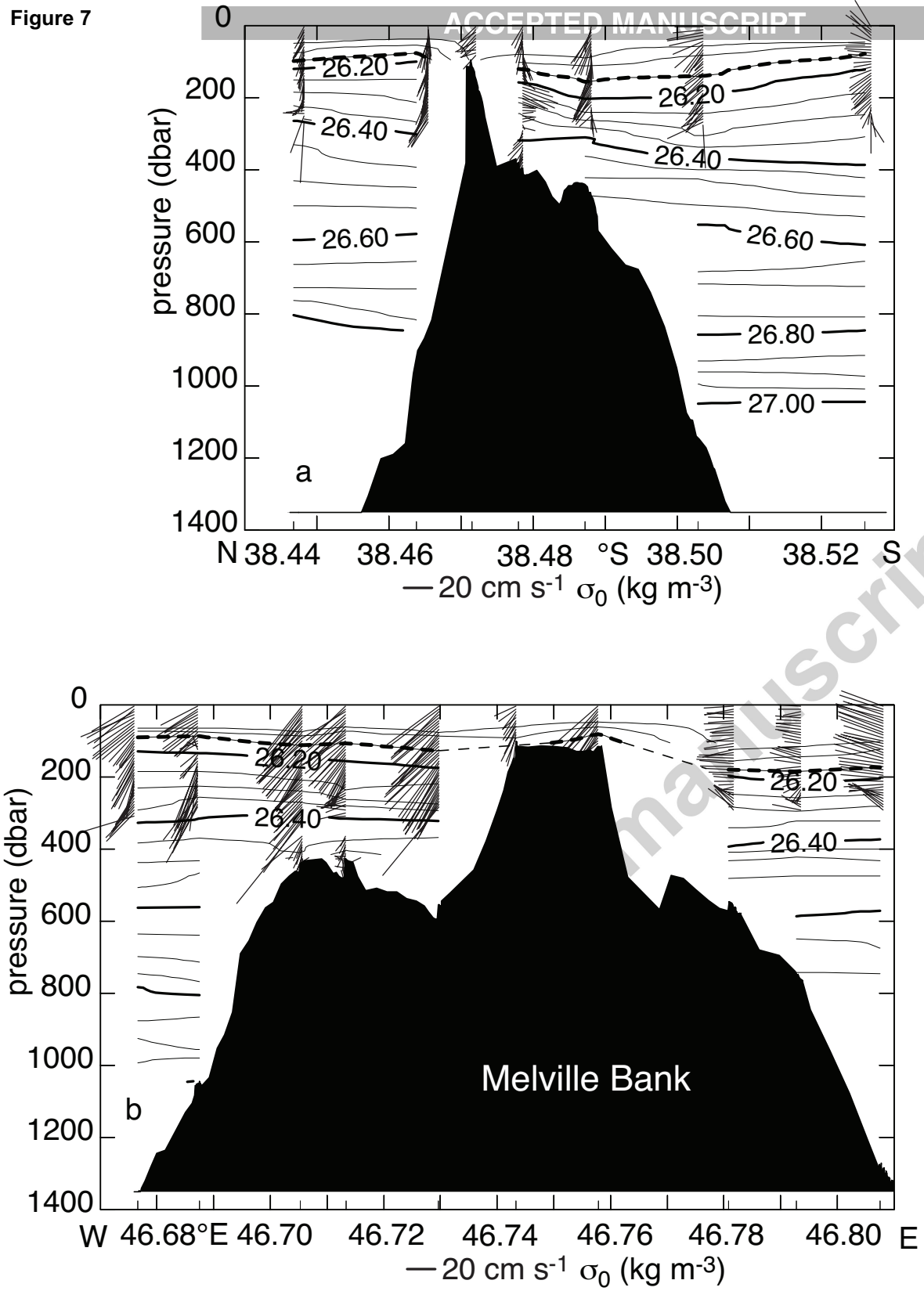

Fig. 7. a) north-south and b) west-east density contours across Melville Bank. Current vectors are from vessel-mounted ADCP measurements, x and y axes are east and north velocity. Short tick marks on the x axes indicate CTD station position.

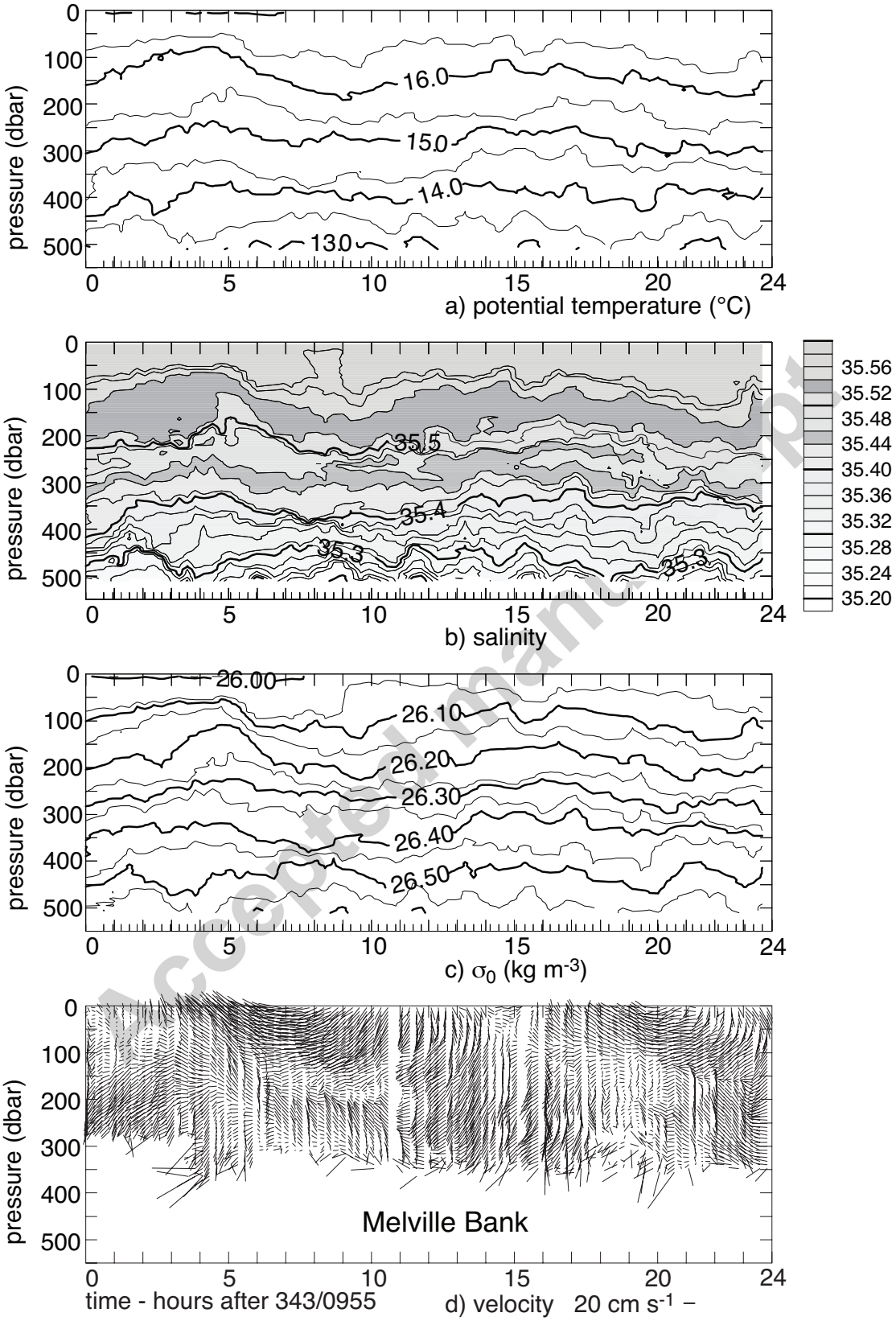

Fig. 8. Melville Bank a) potential temperature, b) salinity, c) density and d) velocity measured over 24 hours starting at day 343/0955, 9 December 2009 at Melville Bank. Velocity x and y are east and north coordinates.

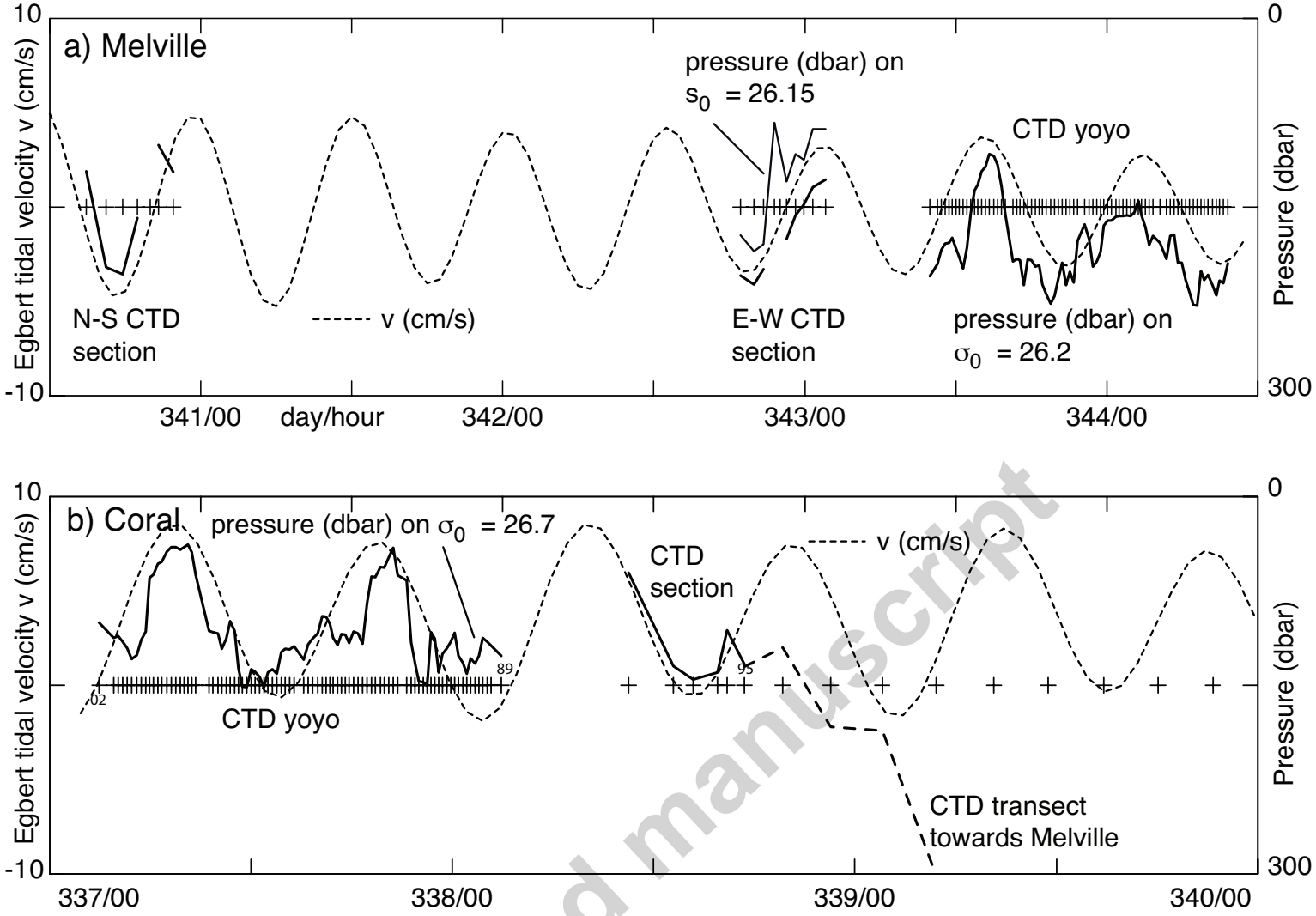

Fig. 9. Isopycnal pressure of (a) 26.2 kg m-3 at Melville Bank and (b) 26.7 m^{-3} at Coral Seamount against time are compared with predicted north velocity (v) from the Egbert tidal model (Egbert and Erofeeva, 2002), dashed line. Individual CTDs are marked +. The CTDs (yoyo and sections) at each site were all within a circle of 5 km radius. The start of the CTD transect from Coral to Melville (station spacing 32 km) is shown dashed in b), demonstrating that spatial variations dominate tidal variations for scales > 30 km. A short section of isopycnal 26.15 kg m^{-3} at Melville shows the anomalously shallow (relative to the tide) dense cap (the spike) over the seamount.

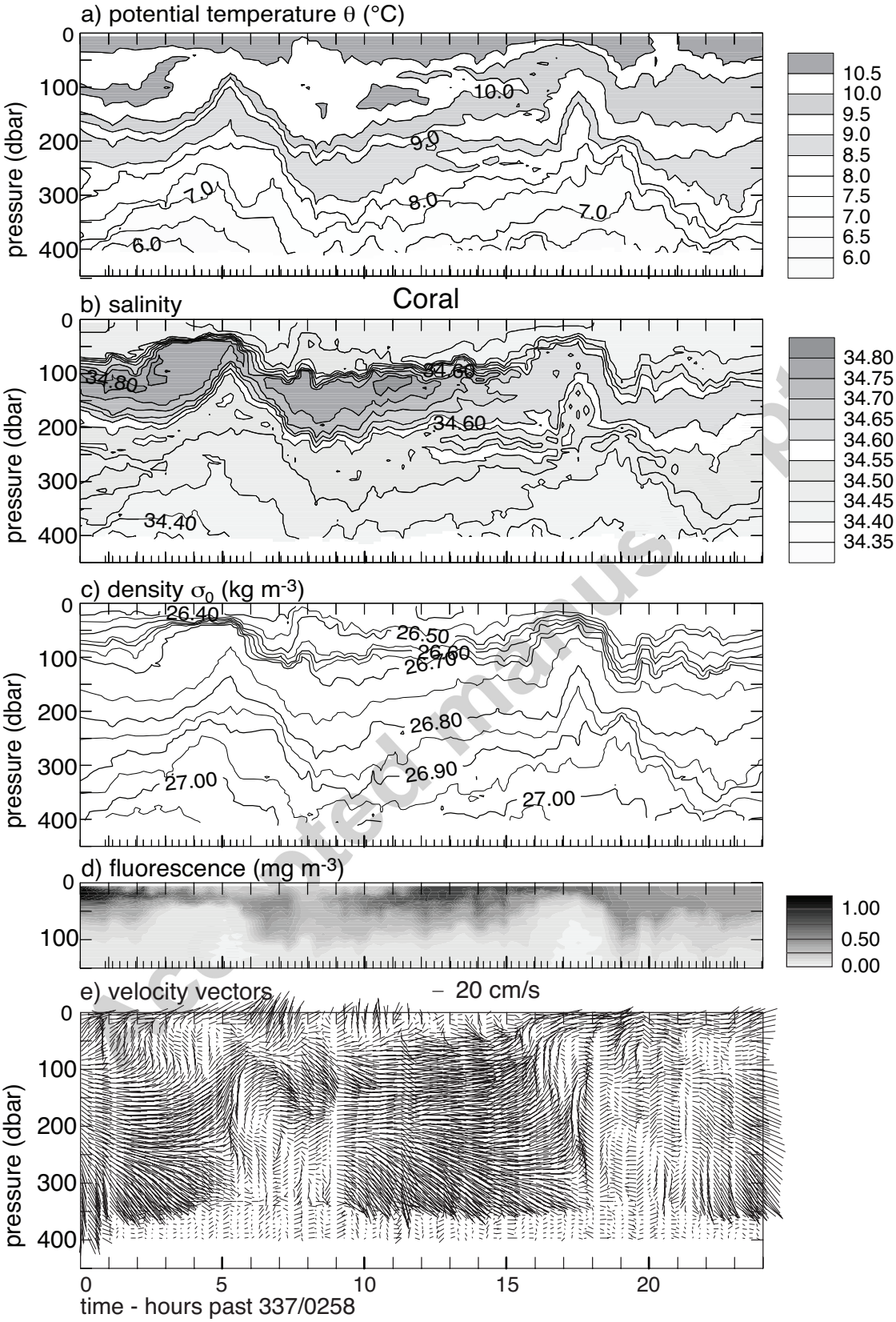

Fig. 10. Coral Seamount a) potential temperature (0.5°C contours), b) salinity (0.05 contours), c) density σ_0 (0.05 kg m^{-3} contours), d) fluorescence (monotonic grey shades) and e) velocity measurements over a 24-hour period (x and y axes are east and north coordinates). Time is shown in hours past the start time, day 337/0258, 3 December 2009

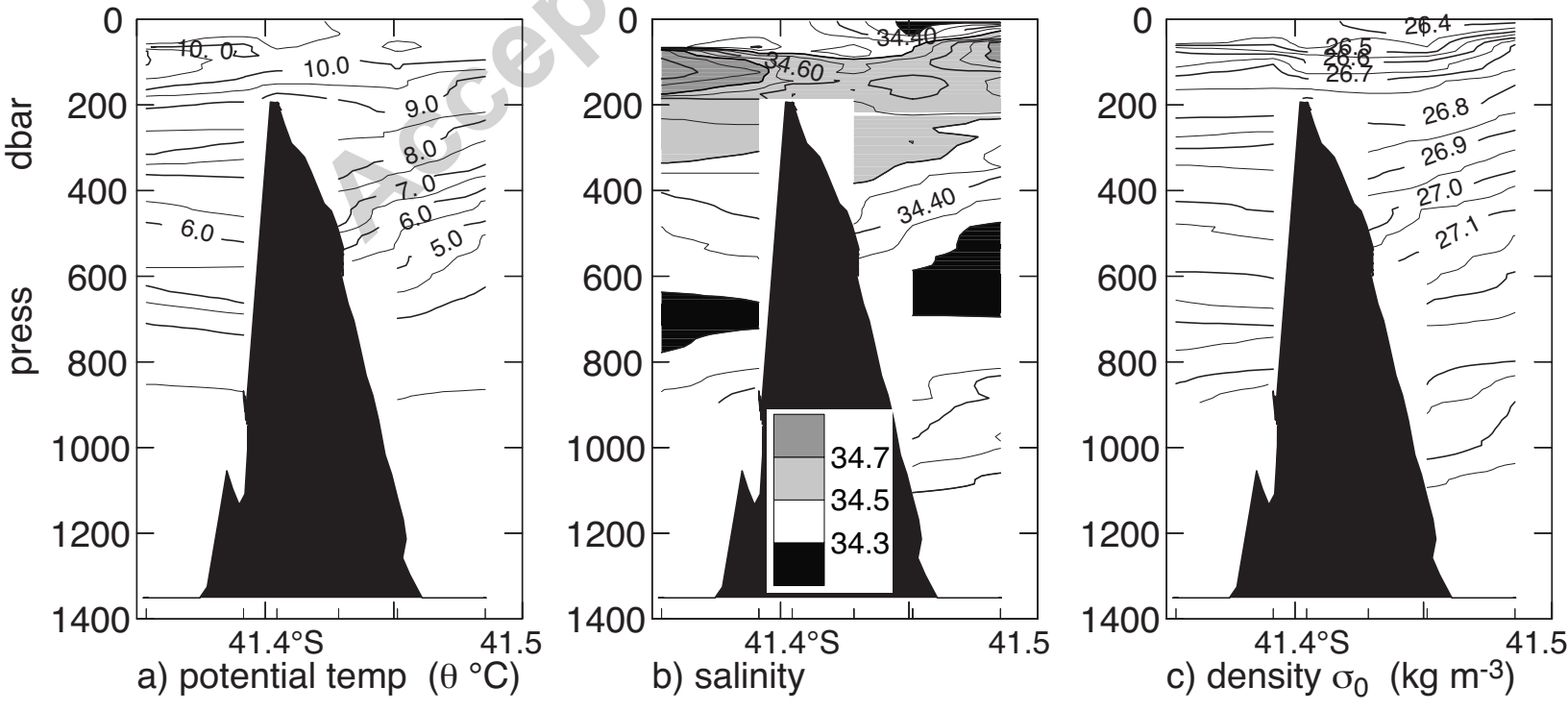

Fig. 11. CTD section across Coral Seamount, a) potential temperature, b) salinity and c) density referenced to the surface. Short tick marks on the x axes indicate CTD positions.